Replacement times of a spectrum of elements in the North Atlantic based on thorium supply

Author list, alphabetical after first author: Christopher T. Hayes[1], Robert F. Anderson[2,3], H. Cheng[4,5], Tim M. Conway[6], R. Lawrence Edwards[5], M. Q. Fleisher[2], Peng Ho[1], Kuo-Fang Huang[7], Seth G. John[8], William M. Landing[9], Susan H. Little[10], Yanbin Lu[11], Peter L. Morton[9], S. Bradley Moran[12], Laura F. Robinson[13], Rachel U. Shelley[9], Alan M. Shiller[1], Xin-Yuan Zheng[14]

Abstract

The measurable supply of ^{232}Th to the ocean can be used to derive the supply of other elements, which is more difficult to quantify directly. The measured inventory of an element divided by the derived supply yields a replacement time estimate, which in special circumstances is related to a residence time. As a proof of concept, Th-based supply rates imply a range in the replacement times of the rare earth elements (REEs) in the North Atlantic that is consistent with the chemical reactivity of REEs related to their ionic charge density. Similar estimates of replacement times for the bioactive trace elements (Fe, Mn, Zn, Cd, Cu and Co), ranging from <5 years to >50,000 years, demonstrate the broad range of elemental reactivity in the ocean. Here, we discuss how variations in source composition, fractional solubility ratios or non-continental sources such as hydrothermal vents lead to uncertainties in Th-based replacement time estimates. We show that the constraints on oceanic replacement time provided by the Th-based calculations are broadly applicable in predicting how elements are distributed in the ocean and for some elements, such as Fe, may inform us on how the carbon cycle may be impacted by trace element supply and removal.

[1] School of Ocean Science and Technology, University of Southern Mississippi, Stennis Space Center, MS, USA
[2] Lamont-Doherty Earth Observatory and Palisades, Columbia University, Palisades, NY, USA
[3] Department of Earth and Environmental Sciences, Columbia University, New York, NY, USA
[4] Institute of Global Environmental Change, Xi'an Jiaotong University, Xi'an, China
[5] Department of Earth Sciences, University of Minnesota, Minneapolis, MN, USA
[6] College of Marine Science and School of Geosciences, University of South Florida, St. Petersburg, FL, USA
[7] Institute of Earth Sciences, Academia Sinica, Taipei, Taiwan
[8] Department of Earth Sciences, University of Southern California, Los Angeles, CA, USA
[9] Department of Earth, Ocean and Atmospheric Science, Florida State University, Tallahassee, FL, USA
[10] Department of Earth Science and Engineering, Royal School of Mines, Imperial College London, London, UK
[11] Earth Observatory of Singapore, Singapore, Republic of Singapore
[12] College of Fisheries and Ocean Sciences, University of Alaska, Fairbanks, Alaska, USA
[13] Department of Earth Sciences, University of Bristol, Bristol, UK
[14] Department of Geoscience, University of Wisconsin, Madison, Wisconsin, USA

1. Introduction

The ocean is a dynamic chemical reactor. The quantity of a particular element in the ocean is the result of a balance between the rates of its supply and removal mechanisms (Barth, 1952; Broecker, 1971). For instance, most major components of sea salt are added slowly from river inflow and removed by the occasional evaporation of isolated seas. By comparing the rate of river inflow of salt to the inventory, or total amount, of salt in the ocean, one derives a replacement time (Berner and Berner, 2012), or how long it would take this source to replace all of the ocean's salt. In a steady-state system where, over some geographical or temporal average, the supply rates and removal rates are equal, replacement time is equivalent to residence time. Residence time is an often-used concept in environmental studies, and its definitions vary (e.g., Bolin and Rodhe, 1973), including how quickly the component cycles through the system or on what timescales we might expect variations in the concentration of this component. Because in general the steady-state assumption is difficult to satisfy, in this study we emphasize the more general concept of a replacement time.

The replacement times (or residence times) of trace elements are difficult to constrain for two reasons. First, especially for contamination prone-elements, there had been a lack of globally-distributed measurements to define their inventories. Secondly, parameters used to estimate elemental fluxes, such as input rates, are challenging to measure directly, and often a small number of discrete flux measurements were extrapolated over the global ocean. This has hindered our ability to accurately model the marine cycling of these elements. A metric for defining how these models treat Fe cycling, for instance, is to produce a global ocean Fe residence time by comparing the ocean Fe inventory to total sources in the model (which are set to equal their sinks, so in this case residence time and replacement would be equivalent). However, available global ocean biogeochemistry models produce Fe residence times that range over 2 orders of magnitude, 4 to 560 years (Tagliabue et al., 2016). This highlights the present uncertainty associated with this essential bioactive trace element's biogeochemical cycle.

Here, we use a technique to estimate trace element replacement times based on dissolved thorium (Th) isotope and trace element measurements from a GEOTRACES zonal section of the North Atlantic (GA03). Such temporal information is critical for understanding the ocean's role in the Earth system, in particular for understanding the distribution and cycling of the micronutrient trace elements whose availability impacts primary productivity and thus the uptake of CO_2 into the ocean (Morel and Price, 2003; Tagliabue et al., 2014). Elements with very short replacement times (decades or less) could display biogeochemical responses to changes in trace element supply or removal that are observable on human timescales (decades to centuries).

The long-lived Th isotopes are scavenged from the ocean by adsorption onto sinking particles on time scales of years to decades, much faster than their rate of radioactive decay (half-life of ^{232}Th = 14.1×10^{9} yr; half-life of ^{230}Th = 75.6×10^{3} yr). Since the source of ^{230}Th in the ocean, decay of dissolved ^{234}U, is well-known and homogeneously distributed, we can use the oceanic distribution of ^{230}Th to quantify a rate of Th scavenging, or the inverse of the residence time with respect to scavenging (τ_{Th} in Eq. 1). In the case of ^{230}Th, its residence time with respect to scavenging is equivalent to its replacement time with respect to production via uranium decay. In support of this statement, it has been shown in models and observations that at any given water column in the ocean, scavenging removal is within 30% of production due to uranium decay (Hayes et al., 2015a; Henderson et al., 1999).

Common Th, ^{232}Th, is supplied to the ocean by continental material, such as mineral aerosol dust (referred to simply as dust in this manuscript) or seafloor sediments (Bacon and Anderson, 1982), and is assumed to be scavenged at the same rate as ^{230}Th. By making a steady-state assumption for the level of ^{232}Th in the ocean, ^{232}Th scavenging rates must be matched by supply of ^{232}Th by the partial dissolution of continental material (Hayes et al., 2013; Hirose and Sugimura, 1987; Hsieh et al., 2011; Huh and Bacon, 1985). The ocean residence time of dissolved Th based on ^{230}Th inventories in the upper 4 km of the GA03 section ranges from 14-28 years across the basin (Hayes et al., 2015a). Given this short residence time, it is likely that the steady-state assumption holds for ^{232}Th throughout most of the ocean, and its

replacement time due to continental material dissolution is likely equivalent to its residence time with respect to scavenging. Using these assumptions, one can derive a dissolved ^{232}Th flux supplied to the ocean simply by measuring dissolved ^{230}Th and ^{232}Th inventories in the ocean (Eq. 1).

Combining Th residence times with the measured dissolved ^{232}Th inventories produces an estimate of dissolved ^{232}Th flux, F(^{232}Th), as a function of integration depth (Figure 1; Eq. 1; see (Hayes et al., 2017) for more details). In Eq. 1, there is more than one way to provide consistency between units among these terms, but here we give one way with each term followed by an appropriate unit. First, ^{232}Th inventories are calculated by integrating ^{232}Th concentrations, resulting in a molar amount of ^{232}Th per square meter. The τ_{Th} in the denominator, in years, on the right hand side of the equation, results from taking the integrated production of ^{230}Th by ^{234}U decay, in this case given in units of ^{230}Th radioactivity, Bq per square meter per year, and dividing by the integrated inventory of ^{230}Th, also in units of radioactivity. In these units, the integrated ^{230}Th production would be simply, $\lambda_{230}{}^{234}$U, where ^{234}U concentration is also in units of Bq, the decay constant λ_{230} being about 9.17×10^{-6} yr^{-1}.

$$F(d^{232}Th) = \frac{\int_0^z d^{232}Th\ dz\ [\frac{mol}{m^2}] \times \int_0^z (\lambda_{230}{}^{234}U) dz\ [\frac{Bq}{m^2 \times yr}]}{\int_0^z d^{230}Th\ dz\ [\frac{Bq}{m^2}]} = \frac{\int_0^z d^{232}Th\ dz\ [\frac{mol}{m^2}]}{\tau_{Th}\ [yr]} \qquad \textbf{Eq. 1}$$

Next, one can derive the flux of another dissolved element, using the generic element Z, coming from the same source, F(Z), using Eq. 2a. To do this, the input ratio of the element to Th of the dissolved phase associated with a particular source must be known, $(Z/Th)_{Input}$. Note for convenience, in Eq. 2 and subsequent equations, we have dropped the 'd' to denote the dissolved phase. For the remainder of the manuscript, when referring to fluxes, replacement time or residence time of thorium or other metals, we are referring to those of the dissolved phase, unless otherwise noted.

$$F(Z) = F(^{232}Th) \times \left(\frac{Z}{Th}\right)_{Input} \qquad \textbf{Eq. 2a}$$

$$F(Z) = F(^{232}Th) \times \left(\frac{Z}{Th}\right)_{UCC} \times \left(\frac{S_Z}{S_{Th}}\right) \qquad \textbf{Eq. 2b}$$

In the case of dust, this input ratio could be defined as the Z/Th ratio of leachates of collected dust samples. In the case of another potential source, such as sediment porewater, one could define the $(Z/Th)_{Input}$ based on the ratio of the elements measured in the dissolved phase of collected porewater samples. However, at present, the Z/Th ratios of sediment porewaters are not well known. In a more general case, an assumption could be made as to the solid phase element to Th ratio, say, for example, using the average composition of the upper continental crust (UCC). Then this solid phase ratio would be multiplied by the relative fractional solubility of Z and Th. Fractional solubility of Z, S_Z, can also be defined by leaching experiments, in which the amount of Z that is leached from the source material is compared to the total amount of Z in the solid material used in the leach, expressed as a percentage. Relative fractional solubility of Z to Th (S_Z/S_{Th}) is therefore the ratio of the fractional solubility for the two elements. Since Th is supplied to the ocean from both dust and seafloor sediment dissolution, in this study we will use the more general case of Eq. 2b. This equation uses the UCC as a source which subsumes two distinct sources (dust and seafloor sediments). If more were known about the Z/Th ratios of the benthic flux, it could be considered separately, but in the absence of that information, we use the simplification that the composition and relative solubility of both dust and seafloor sediments are the same. Of course, many elements have important sources whose composition significantly differs from the UCC (e.g., rivers, groundwater, etc.), this is nonetheless our starting point.

The goal in deriving these elemental fluxes is to compare them with measured inventories to derive replacement times. We emphasize here that our Th-based approach will not account for some other important sources to the ocean, such as hydrothermal vents. Additionally we are making no assessment of how our supply rates compare to the removal rates or otherwise assessing the steady state assumption. For instance, dissolved Fe can be removed from the ocean in a number of ways including scavenging, biological uptake, or inorganic precipitation (Tagliabue et al., 2017). If the sum of these removal terms were equal to our supply estimate based on ^{232}Th fluxes at steady-state, the derived replacement time would be equivalent to a residence time. Rather than assess that equivalency here, we can use the more

limited replacement time concept as a way to view the relative rates of temporal cycling of a broad array of elements that have been measured in the GEOTRACES program.

We can anticipate that our replacement times will overestimate the residence time if there are sources of the elements of interest that are not accounted for by the dissolved ^{232}Th flux calculated for the North Atlantic. The sources of ^{232}Th to the North Atlantic are largely dust deposition and margin sediment dissolution. Other sources of trace elements to the North Atlantic may include hydrothermal venting, rivers, estuaries in which riverine sources can be diminished (Andersson et al., 1995; Boyle et al., 1977) or enriched (Shiller, 1997), submarine groundwater discharge, and/or water masses that advect a dissolved signal derived from processes occurring at or before their point of origin (preformed signature). At steady state all these sources will be equal to the sum of removal fluxes, again written in the form of the tracer conservation equation for the generic dissolved element, Z, in Eq. 3.

$$\frac{dZ}{dt} = F(AD) + F\left(^{232}Th\right) \times \left(\frac{Z}{Th}\right)_{input} + F(vents) + F(rivers) - F(scav) - F(biol) - \cdots = 0$$

Eq. 3

Here, F(AD) represents the sum of advective and diffusive circulation fluxes into or out of the "box" of ocean in question, F(vents) represents source from hydrothermal vents, F(rivers) the source from rivers, F(scav) represents removal by scavenging, F(biol) represents removal by biological uptake, and there may be many other terms in the full balance not accounted for here (represented by "…" in Eq. 3).

Rearranging Eq. 3, we can estimate the replacement time of dissolved element Z, τ_Z, by dividing the inventory, or total amount, of dissolved Z in the ocean "box" in question, by the sum of its source terms (Eq. 4). Inventories are calculated by integrating dissolved elemental concentrations with depth from the surface downward.

$$\tau_Z = \frac{inventory\ of\ Z}{F(AD)+F\left(^{232}Th\right)\times\left(\frac{Z}{Th}\right)_{Input}+F(vents)+F(rivers)} \qquad \textbf{Eq. 4}$$

Since the residence time of Th (decades) is much shorter than the transit time of deep ocean water masses (centuries to millennia), Th measured along GA03 likely has little preformed component. Thus, in considering water column inventories of Th, advective and/or diffusive sources can be neglected. Longer residence time elements, however, may have a substantial or even dominant preformed component. Thus, if F(AD) is a substantial flux for element Z, or similarly if F(vents) is large compared to the Th-based supply, then the replacement time we calculate by Th-supply alone will overestimate the residence time. By making an area-weighted average of all the stations occupied on GA03, and assuming these stations represent the entire North Atlantic, the preformed supply of elements from North Atlantic water masses will be accounted for. Supply from outside the North Atlantic (e.g., Antarctic Bottom Water), however would still be unaccounted for. Furthermore, if our estimate of $(Z/Th)_{Input}$ is higher or lower than the true value then our replacement times will underestimate or overestimate the residence time, respectively. In the case of using the Eq. 2b for input term, our estimate of either $(Z/Th)_{UCC}$ or S_Z/S_{Th} could be biased higher or lower than the true value.

2. Methods

2.1 *Data sources*

We draw upon data from previous GA03 publications of dissolved ^{230}Th (Hayes et al., 2015a), Fe (Conway and John, 2014a; Hatta et al., 2015), Zn (Conway and John, 2014b; Roshan and Wu, 2015a), Al (Measures et al., 2015), Mn (Wu et al., 2014), Cd (Conway and John, 2015; Wu and Roshan, 2015), Cu (Jacquot and Moffett, 2015; Roshan and Wu, 2015b), and Co (Noble et al., 2017). We also use data from leaching experiments performed on aerosol material collected during the cruise (Shelley et al., 2018). Data from this transect on ^{232}Th, yttrium and the rare earth elements (REE) are presented here for the first time. Methods to determine dissolved ^{232}Th were reported by Hayes et al. (2015a). Y and REE were determined by a combination of isotope dilution and external standard mass spectrometry and detailed methods are reported by Shiller (2016a). Full section views of the Y and REE concentration sections are available at http://egeotraces.org. All GA03 data are accessible through the Biological and Chemical

Oceanography Data Management Office (http://data.bco-dmo.org/jg/dir/BCO/GEOTRACES/NorthAtlanticTransect/) or the GEOTRACES Data Products (Mawji et al., 2015).

2.2 *Rare earth element composition and solubility*

For calculating REE replacement times, using Eqs. 3 and 4, we define $(REE/Th)_{UCC}$ based on two sources (Table 1). A published synthesis (Rudnick and Gao, 2014) defines the average values for the upper continental crust and a GA03 aerosol study (Shelley et al., 2015) defines end-member elemental ratios of North African dust, likely a major source of Th and REEs to this section. Both of these estimates are used in our calculations as a way of taking into account uncertainty in the source material ratios. Most of the REE/Th ratios are similar (within 30%) for the two estimates, except notably for Gd, Tb, Tm and Lu. North African dust has a factor of 2 or more greater REE:Th ratio than the average UCC for these elements.

To define the relative fractional solubility of REEs to Th, we use results from aerosol leaching experiments of North African dust samples collected on GA03 (Shelley et al., 2018). Two types of leaches were performed on aerosol samples that were designed to represent a range in leaching intensity that continental particles experience under oceanic conditions: (1) an ultrapure (18.2 MΩ) deionized water leach (DI leach) (Buck et al., 2006) and (2) a pH 2 leach consisting of 25% acetic acid and 0.02 M hydroxylamine hydrochloride with a 10 minute heating step at 90–95°C (Berger et al., 2008) (HAc leach). In general, absolute fractional solubility values defined by leaching experiments have been found to be highly sensitive to experimental conditions (Morton et al., 2013). In the present study, however, only the relative fractional solubility between an element and Th is used (Eq. 3), and relative fractional solubility may be less sensitive to leach method. For example, it was found that S_{Th} was an order of magnitude larger in the HAc leach compared to DI leach (Anderson et al., 2016), while REE fractional solubility relative to that of Th (S_{REE}/S_{Th}) differ between the two leaches by less than 30% (except for Ce, for which the HAc leach gave a 40% higher value than the DI leach) (see Table 1). One previous study determined

188 S_{REE}/S_{Th} for in-situ pumped lithogenic particles from the Mediterranean Sea for La, Ce, Pr, Nd, Gd, Dy,
189 and Er, by incubating the filtered particles in seawater containing endemic bacteria under oxic conditions
190 in the dark for several days (Arraes-Mescoff et al., 2001). This study found similar S_{REE}/S_{Th} values as
191 those reported here, averaging 3.8 ± 1.7 (avg. ± 1 s.d., n = 11) for all REEs studied, displaying no
192 apparent trend with atomic number. Interestingly, the HAc leach values for S_{REE}/S_{Th} are consistently
193 higher than those of the DI leach (Table 1). Here to account for the uncertainty in residence time
194 estimates induced by different leaching techniques, we have used fractional solubility ratios from both the
195 DI leach and HAc leach in calculations.

196 ***2.4 Bioactive trace element composition and solubility***

197 For the bioactive elements considered here (Mn, Fe, Co, Cu, Zn, Cd) and Al, often used as an
198 abiotic analogue for the scavenged-type trace metals, we also use both UCC and North African dust
199 metal:Th ratios (Rudnick and Gao, 2014; Shelley et al., 2015) as a way to account for variability in source
200 material (Table 2). These sets of ratios also are generally consistent with each other, except notably for Zn
201 and Cd for which the North African dust metal:Th ratio is highly elevated compared to the UCC. We take
202 this comparison with caution because it is possible the North African dust estimates may contain Zn
203 and/or Cd contamination from co-occurring anthropogenic emissions (Grousset et al., 1995; Shelley et al.,
204 2015). Furthermore, as discussed further below, for some of these elements, rivers are likely the dominant
205 source, instead of dust, to the North Atlantic. While the element to Th ratios in global rivers has been
206 estimated (Gaillardet et al., 2014) (Table 2), one could not use them to estimate riverine elemental supply
207 without having a good constraint on the flux of Th from rivers alone. Additionally, element to Th ratios
208 are likely modified in estuarine processes. Thus, we realize that making a replacement time estimate of
209 river-supplied elements like Cd based on the sources that supply Th (dust and sediment dissolution) is
210 apparently “mis-matched”. Nonetheless, the comparison of the apparent results for these types of
211 elements to the elements with sources more similar to Th is still useful in demonstrating the relative range
212 of possible replacement times in the ocean.

213 The relative solubility will again be a major source of uncertainty for the bioactive trace metals.
214 There are few studies which determine the relative solubility of all the elements of interest here. In
215 particular oceanic Th fractional solubility data is rather limited and ranges from about 1-29%, in
216 published work (Anderson et al., 2016; Arraes-Mescoff et al., 2001; Hayes et al., 2017; Robinson et al.,
217 2008; Rowland et al., 2017; Roy-Barman et al., 2002). Based on time-series measurements of Th and Fe
218 at Station ALOHA (Hayes et al., 2015b), it is likely that S_{Fe}/S_{Th} is close to 1, but this may vary regionally
219 and episodically. However, broadly consistent with that finding, DI and HAc leaches of the North African
220 dust aerosols from GA03 produced S_{Fe}/S_{Th} estimates of 0.4 ± 0.2 (n=2) and 1.3 ± 0.3 (n=15), respectively.

221 Mn, Al and Co have either predominant or significant sources from atmospheric deposition to the
222 North Atlantic basin (Measures et al., 2015; Noble et al., 2017; Wu et al., 2014). The DI leach results for
223 S_{Mn}/S_{Th} were very variable (3841 ± 804, n = 2). Thus, here, we rely more heavily on the HAc leach for
224 S_{Mn}/S_{Th} (9.8 ± 2.4, n = 7). DI and HAc leaches produced relative solubility ratios consistent with each
225 other within uncertainty for Al (S_{Al}/S_{Th} ~ 2) and Co (S_{Co}/S_{Th} ~ 6).

226 As mentioned above, the sources of Cd, Cu and Zn are likely dominated by rivers (Little et al.,
227 2015) and not atmospheric deposition. However, since we are defining replacement times with respect to
228 the sources that supply Th, it is still appropriate to define the relative element to Th solubility in the
229 sources that supply Th (namely, atmospheric deposition and sediment dissolution). The DI leach of
230 Saharan aerosols for Zn/Th was highly uncertain (S_{Zn}/S_{Th} = 20 ± 19, n = 2), while its HAc leach was
231 better constrained (S_{Zn}/S_{Th} = 6.7 ± 3.5, n = 7). Similarly, DI leaches for Cd/Th and Cu/Th were more
232 variable but were consistent with the HAc leach within uncertainty (S_{Cd}/S_{Th} ~ 10 and S_{Cu}/S_{Th} ~ 3). Again
233 if the Th-based supply of Cd, Cu and Zn underestimates the total supply of these elements (Eq. 4), the
234 replacement times we derive will be overestimates of the residence time.

235 **3. Results**

236 ***3.1 ^{232}Th distribution, flux and sources***

The distribution of dissolved ^{232}Th across the Woods Hole-Mauritania portion of GA03 is shown in Figure 1. Near the Mauritanian margin, dissolved ^{232}Th concentrations are elevated throughout the water column due to North African dust deposition (Anderson et al., 2016) and, to some extent, due to input from margin sediments. The dissolved ^{232}Th distribution has similarities with that of the isotopic composition of dissolved Fe (δ^{56}Fe; Fig. 1), indicative of a common source of these lithogenic metals. At the four easternmost stations, the dissolved Fe was characterized by lighter δ^{56}Fe values (compared to the continental crust) throughout much of the water column. Conway and John [2014a] ascribed this signal to a mixing of Fe sources of roughly 80–90% dissolution from aerosol dust (with a hypothesized isotopically heavy signature (Conway and John, 2014a; John and Adkins, 2012) and 20–10% reducing margin sediments (with an isotopically light signature due to dissolved Fe(II) release from reducing porewaters (Severmann et al., 2006)) . Because of Th's similar distribution in concentration space to δ^{56}Fe, a similar balance of sources may exist for Th. Future work may be able to independently constrain a margin sediment source of Th using the potentially quantifiable source of ^{228}Ra from the sediments (Charette et al., 2016).

Much of the deep Atlantic basin has a background dissolved ^{232}Th concentration of 0.2–0.3 pmol/kg, with a marked depletion around the Mid-Atlantic Ridge, a signal of intense Th scavenging (Hayes et al., 2015a) in waters impacted by hydrothermal plumes (indicated on Fig. 1 by a light excursion in dissolved δ^{56}Fe from hydrothermal iron input). In the northwestern Atlantic, Upper Labrador Seawater, seen in the section plot around 1200 m depth from section distance 500 to 2000 km, is characterized by elevated ^{232}Th (0.3-0.4 pmol/kg), and similarly traced by lighter (near-crustal) dissolved δ^{56}Fe compared to the background basin (Fig. 1). In the case of Upper Labrador Seawater, Conway and John (2014a) ascribed the sources of dissolved Fe as 70-90% non-reductive sediment release and 30-10% aerosol dust. The seafloor sediments in the region of Labrador Seawater formation are of upper continental crust origin, and they may face leaching-type conditions even more intense than in the water column from sediment resuspension and burrowing activity (Aller and Aller, 1986). Thick nepheloid layers were seen in this

portion of the GA03 section (Lam et al., 2015). Thus, ^{232}Th may be a general tracer for continental material in the ocean, whether leached from dust or seafloor sediments.

Finally, in the upper 500 m of the section between Woods Hole and Bermuda, elevated ^{232}Th is seen in waters influenced by the Gulf Stream, consistent with previous observations off Cape Hatteras (36.1°N, 74.4°W) (Guo et al., 1995). In this case of the Gulf Stream, elevated ^{232}Th concentrations appear de-coupled with changes in Fe isotopic composition in contrast to the rest of the section, likely because the Gulf Stream is carrying a signal from its source regions further south.

3.2 REE replacement times as proof of concept

We begin with a focus on rare earth elements and yttrium (in this paper we include Y when using the abbreviation REE, sometimes abbreviated as YREE) because their ocean geochemical cycles may be similar to that of Th, with supply by upper continental crustal material (including dust, riverine particles or seafloor sediments) and removal by adsorption onto sinking particles, or scavenging (Elderfield, 1988). Additionally, REEs have generally decreasing particle-reactivity with increasing atomic number. This is related to their similar valence state (3+) and decreasing ionic size with increasing atomic number. REE scavenging in seawater has been studied in detail (Byrne and Kim, 1990; Quinn et al., 2004; Schijf et al., 2015), and a gross simplification can be made that increased ionic charge density for the heavier REEs means they are more strongly complexed in seawater by carbonate ions and thus less susceptible to scavenging. Anomalous to the overall trend, seawater has low Ce/REE ratios in comparison with the UCC since Ce can exist in either the 3+ or 4+ state, the latter being much more insoluble in seawater.

The calculated replacement times of the dissolved REEs are presented in cross-section form in Figure 2 using North African dust REE/Th composition and HAc leach solubility ratios. An area-weighted average across depth horizons was also calculated to represent the basin-wide North Atlantic replacement time (see Table 1 and Supporting Information for averaging method and tabulated data). Replacement times generally increase with integration depth and with atomic number from roughly 5 to

500 years. The extremes are Y, with the largest of the replacement times, 580 ± 90 years for the whole North Atlantic (error representing uncertainty related to the compositional and solubility ratios), and Ce, being 15 ± 5 years. We note that the derived dissolved Ce replacement time range is roughly half the residence time of dissolved Th, meaning Ce must be relatively intensely scavenged.

For most REEs the replacement time appears to increase with integration depth relatively abruptly in the deep eastern Atlantic basin below 4 km depth, compared with the western basin (Fig. 2). In investigating this pattern, it is worth noting that the Mid-Atlantic Ridge hydrothermal vents are not a source of REEs to the ocean and are actually a sink from scavenging onto hydrothermal particles (Stichel et al., 2018; Zheng et al., 2016). The apparent increase in replacement time in the deep eastern basin therefore may be explained by the presence of preformed REEs transported by Antarctic Bottom Water (AABW). It has been estimated that in the deep waters of GA03 about 20% of the dissolved Nd was added from local sources (dust or sediment dissolution), the other 80% being from preformed water masses (from both the North and South Atlantic) (Shiller, 2016b; Stichel et al., 2015). AABW is about 1.7 times more concentrated in dissolved Nd than lower North Atlantic Deep Water (Zheng et al., 2016). With this information and the estimate that the deep portion of GA03 is 30% AABW (Jenkins et al., 2015a), about 25% of the deep Nd in GA03 may have originated from outside the North Atlantic. Assuming there is no preformed ^{232}Th from AABW, the REE replacement times based on Th supply may overestimate the true North Atlantic residence time, by probably about 25%.

Nonetheless, the trend in replacement times across the spectrum of REEs is quite robust. Taking the basin-averaged replacement times at the 1 km integration depth level, to reduce the effect of preformed supply (although the full water column integration results also give a similar trend), REE replacement times follow a similar trend to REE ionic charge density (Rayner-Canham and Overton, 2006) (Fig. 3). This is consistent with the simple prediction that at higher charge densities (i.e., heavier REEs), a greater fraction of REEs are complexed by carbonate ions, thus less susceptible to scavenging removal (with the exception of Ce). These results support the idea of inorganic complexation increasing

311 REE residence times in the ocean, which is predicted by thermodynamic treatments (Byrne and Kim,
312 1990; Quinn et al., 2004; Schijf et al., 2015).

313 Figure 3 also shows the sensitivity of these replacement time estimates to the choice of
314 compositional and solubility ratios. In particular, the lower Gd/Th ratio of the UCC results in a large
315 positive anomaly in the replacement time estimate, whereas the estimates using the North African dust
316 end-member fall in line with the atomic size trend, suggesting the North African dust end-member is a
317 more relevant source in this area. This results suggests that anthropogenic Gd, sourced from its medical
318 use as a contrast agent in magnetic resonance imaging, may have contaminated both North African dust
319 and the adjacent Atlantic Ocean, as has been observed in the Mediterranean (Censi et al., 2010), the North
320 Sea (Kulaksiz and Bau, 2007) and many other sites.

321 There have been prior REE ocean residence time estimates, most notably for Nd, for comparison
322 with results reported here. Since the isotopic composition of dissolved Nd is a quasi-conservative tracer of
323 water masses in the deep ocean (Tachikawa et al., 2017), it has been inferred that the ocean residence
324 time of Nd must be shorter than the mixing time of the ocean (~1000 years). In our dataset, integrating the
325 whole North Atlantic results in a Nd replacement time of 110 ± 20 years (Table 1, Fig. 4), the uncertainty
326 representing the variation in composition and solubility values chosen. This estimate is shorter than the
327 Nd residence times (200-1000 years) calculated by comparing isotopic composition of particulate Nd with
328 that of the surrounding seawater (Tachikawa et al., 1999). Note as well, as shown in Fig. 3, that if one
329 only considers the upper 1 km, the dissolved Nd replacement time is about 25 years, which is likely
330 shorter than the ventilation timescale of ~40 years (Jenkins et al., 2015b). This suggests Nd is unlikely to
331 trace water mass properties in the upper 1 km of the ocean, in agreement with other studies (Tachikawa et
332 al., 2017). Additionally, a recent Eastern Equatorial Pacific study found significant changes in dissolved
333 Nd isotopic composition through the upper 2.5 km of the water column from station reoccupations
334 separated by only 3 years (2009 and 2012), suggesting a very rapid turnover time (Grasse et al., 2017).

Another study made basin-scale estimates of REE residence times by comparing an estimate of the global seawater inventory with removal by sinking particles (Li, 1991). While these estimates are based on much less data available at the time, they are generally consistent with the lower end of the ranges we calculate using the Th-technique specific to the North Atlantic. More importantly, the trend in residence/replacement time is consistent (Table 1, Fig. 4). This also supports the notion that our replacement time estimates are somewhat overestimated due to lateral REE supply by AABW. Nonetheless, given the consistency in trend with atomic number and the absolute magnitude of the residence times, it appears that the Th-supply based replacement times are relatively well constrained.

3.4 Prior residence time estimates of the bioactive trace elements

In addition to REE, the Th flux-based replacement time approach can be used to estimate the replacement times of bioactive trace elements of interest to marine biogeochemical processes: Mn, Fe, Co, Cu, Zn, and Cd. We also consider dissolved Al residence times in GA03, since Al is often used as the abiotic analogue to the bioactive trace elements. All these elements are measured by GEOTRACES endeavors and are becoming the focus of biogeochemical modelling studies. While the geochemical cycles of these elements involve many biological transformations in which Th does not participate, their main source to the ocean is ultimately from upper continental crust, whether from dust, rivers, groundwater, or margin sediments, excluding hydrothermal inputs. Knowing this, we can proceed to estimate the replacement times of these elements in the same way as for REEs, while highlighting the extent to which this approach is limited. For instance, hydrothermal inputs of these elements will lead the replacement time based on Th supply to overestimate the residence time (since hydrothermal vents supply little Th to the ocean (Pavia et al., 2017). Additionally, as in the case of the REEs, the contribution of preformed elements in AABW may also result in our approach overestimating residence time.

Before discussing our new replacement time estimates, it makes sense to review the best existing estimates of the ocean residence times of these elements (Table 2). There has been much progress in understanding the magnitudes of various trace element sources and sinks. Current best-estimate residence

times for Zn, Cu, Cd, are 8,000–11,000 years (Little et al., 2016), 2,000–3,300 years (Little et al., 2017) and 26,000–55,000 years (Little et al., 2015), respectively, based on full oceanic mass balance calculations. These estimates are based on global sources and sinks, so we emphasize care taken in their comparison to the replacement times derived here, which are specific to the North Atlantic and do not necessarily include all relevant source fluxes. Bruland et al. (1994), deriving a residence time based on removal by sinking particles in the North Pacific, estimated a slightly shorter Zn residence time than the global residence time of Little et al. (2016) of 3,000–6,000 years. The Bruland et al. (1994) method produced a similar residence time estimate as Little et al., (2015) for Cd of 22,000–45,000 years. Finally, Roshan et al. (2016) also calculated a shorter Zn residence time (3000 ± 600 years) than Little et al. (2016), by adding recently observed hydrothermal sources of Zn to the sum of Zn sources compiled by Little et al. In contrast to these relatively long timescales, for Mn, Co and Al, the best available estimates are much shorter than the timescale of deep ocean circulation (20–40 years (Bruland et al., 1994), 40–130 years (Hawco et al., 2017; Saito and Moffett, 2002), and 45–90 years (Bruland et al., 1994), respectively). These estimates are based on scavenging and particle sedimentation, likely the major removal mechanism for these elements.

Constraining the residence time of Fe is an obvious community priority because of Fe's influential role as a key micronutrient in biogeochemical cycles and its consequent role in limiting primary productivity over large regions of the ocean. Thus, understanding how quickly the supply of Fe changes with time is of great significance to the global carbon cycle. Despite this importance, the propensity for Fe to be contaminated during collection and analysis has historically led to challenges in ascertaining Fe concentrations accurately. However, after accruing a larger dataset of uncontaminated Fe analyses, two groups initially developed deep ocean Fe residence time estimates based on the scavenging rates of Fe in deep waters (70–140 years in the deep Pacific (Bruland et al., 1994) and 130–410 years in the deep Atlantic (Bergquist and Boyle, 2006)).

More recently, Hayes et al. [2015c] used the Th supply-based approach described in this study to estimate a deep Pacific Fe residence time near Hawaii of about 30 years. Because of the disagreement with the century-scale residence time estimates, those authors hypothesized that Th supply could somehow be decoupled from Fe supply in the deep ocean, resulting in a significant overestimation of the Fe supply and a residence time estimate that is too low. Recent results from modelling studies, however, are providing some support for the notion that the residence time of Fe may be decadal rather than centennial, or could vary significantly between basins and with different Fe speciation. In the intercomparison of global ocean iron models, 5 of the 13 models recently examined in a review by Tagliabue et al. [2016] gave global Fe residence times of less than 10 years, and 8 gave less than 50 years (average and standard deviation: 145 ± 176 years). Furthermore, Kipp et al. [2017] estimated a residence time of dissolved Fe in the hydrothermal plume emanating from the East Pacific Rise at 2.4 km depth of 9–20 years, based on scavenging rates of Fe in the plume. Thus, while each of these residence time estimates differs somewhat in their approach to defining a residence time, it is clear that there remains significant uncertainty in the residence time of Fe in the ocean.

The replacement times we derive here are specific to the North Atlantic, omit key sources such as hydrothermal vents and rivers, and are not necessarily representative of a steady-state situation. Our comparison of replacement times to globally or regionally defined residence times in the literature is thus not meant to be strictly quantitative.

3.5 Replacement times of the bioactive trace elements estimated with the Th-based approach

Here, we estimate replacement times for the bioactive elements using the Th-based approach on the GA03 dataset, with results shown for Fe, Mn, Al, Co, Zn, Cu and Cd in Figs. 5, 6 and Table 2. The overall range in replacement times of the bioactive elements estimated here for the whole North Atlantic are for the most part consistent with the range of previous residence time estimates (Fig. 5). North Atlantic Zn, Cd and Cu replacement times are close to or longer than the ocean mixing time (>1000 years), while those of Fe, Mn, Co and Al are significantly shorter, decadal or less. Figure 6 shows section

views of the replacement time estimates using UCC composition and HAc leach solubility ratios and Figure 7 shows the area-weighted average depth profile of the North Atlantic replacement times. The errors reported in Fig. 5, 7 and Table 2 take into account uncertainty in the composition and solubility ratios by comparison with results of the calculation using North African dust and DI leach information. Uncertainty related to AABW supply or other "missing" terms in the steady-state budget are not accounted for.

3.6 Upper water column replacement times of the bioactive trace elements

While the focus of this manuscript is North Atlantic basin-scale replacement times, the Th-supply method can be used at any integration depth and may indeed be quite useful in interpreting bioactive trace element behavior in the euphotic zone, as shown in the shallow portions of the section plots of Fig. 7. These estimates, expanded for more detail in the upper 1 km m are presented with limited discussion in the Supporting Information for Fe, Mn, Al, Cu, Zn, Cd and Co. In the upper water column, especially for elements with short residence times, rivers and preformed elements are much less likely to be significant contributors to the measured inventories. Therefore, in the upper ocean the Th-based approach may give a more reliable estimate of element replacement time specifically by dissolution of dust, as has been argued for Fe (Hayes et al., 2015b). On the other hand, in considering the upper ocean alone, another potential source of elements may need to be considered, which is the upwelling of water with Z/Th ratios distinct from dust. A significant upwelling source may be limited to upwelling regions such as the Mauritanian margin, and thus basin-wide averaging is likely to reduce the bias introduced.

Lastly, with available GEOTRACES data, we can make both upper ocean and deep ocean replacement time estimates for Sc, V, Ni, Ga, and Ba. These estimates are also given in the Supporting Information.

4. **Discussion**

Our North Atlantic Fe replacement time of 6 ± 3 years is more similar to previous decadal or shorter estimates of residence time (Hayes et al., 2015b; Kipp et al., 2017; Tagliabue et al., 2016) than the century-scale estimates (Bergquist and Boyle, 2006; Bruland et al., 1994). In making these comparisons, it is worth noting that our Th-based Fe replacement time could underestimate the residence time if the true value of S_{Fe}/S_{Th} is less than ~0.5–1.3. However, the true S_{Fe}/S_{Th} value would have to be less than 0.05 to produce a century-length dissolved Fe replacement time. Of course, different regions of the ocean are likely to be characterized by different effective relative solubility ratios because of different chemical conditions or distinct sources (Fig. 1). For instance, Fe could be much more effectively leached from dust than Th in surface waters due to biological activity, photoactivity, easily-weathered surface oxide coasting, and/or ligand influences. In contrast, in abyssal waters, Th could continue to be leached where there is less Fe released (thus S_{Fe}/S_{Th} could be higher in surface waters and lower in deep waters). Different organic ligands and ambient conditions could also play a role. Such water-column variability is not considered in our calculation here; however, the relative solubility number represents the integrated dissolution of both elements throughout the water column, whatever the depth profile of relative solubility might look like. The true integrated S_{Fe}/S_{Th} would thus again need to be quite low to produce a centennial replacement time in this case.

The very short North Atlantic replacement time for Mn (5 ± 1 years) implies rapid removal by processes such as biological uptake, oxidation and/or particle scavenging. Nonetheless, if the true S_{Mn}/S_{Th} value were less than ~10 as used here, our replacement time estimates would increase, perhaps to be more in line with the previous residence time estimate of 20-40 years (Table 2). It might be that in leaching experiments, relative Mn/Th solubility is greater than what would occur in situ in the ocean. Further investigation into how relative solubility ratios change in different leaching methods may shed light on this issue.

The North Atlantic replacement time for Co in this analysis (140 ± 70 years) is similar to the best previous residence time estimates (Hawco et al., 2017; Saito and Moffett, 2002). Additionally, Al has a

457 deep ocean replacement time of 50 ± 10 years, again broadly consistent with previous residence time
458 estimates (Bruland et al., 1994; Chester and Jickells, 2012) and being slightly longer than the residence
459 time of Th, also expected based on previous work (e.g., (Moran and Moore, 1989)). The mid-ocean ridge
460 in the vicinity of GA03 may be a source of Al, either from hydrothermal input (Measures et al., 2015) or
461 sediment dissolution on the flanks of the ridge (Middag et al., 2015), and either source would contribute
462 to our replacement time overestimating the true residence time here.

463 The hydrothermal plume at the GA03 Mid-Atlantic Ridge is clearly a large source of Fe and Mn
464 (Conway and John, 2014a; Hatta et al., 2015) which would not be accounted for by Th-based estimates of
465 Fe and Mn supply. The Th-based dissolved Fe flux at the depth of the hydrothermal plume in GA03 is
466 about 640 μmol/m^2/yr. The Th-based dissolved Fe replacement time rises to 30 years in the plume,
467 compared to 5 years at the same depth in surrounding stations (Fig. 6). In the basin-averaged data (Fig. 7),
468 the full magnitude of this anomaly is partly averaged out, but an increase at the depth of the ridge crest
469 (~3500 m) is still apparent. If the overall Fe residence time should be 5 (rather than 30) years in the deep
470 North Atlantic, then the Fe flux at the ridge site would have to be six times larger than the Th-based
471 estimate, implying about 3200 μmol/m^2/yr of hydrothermal Fe being added (see Eq. 4). This is much
472 higher than our current best estimates of the hydrothermal Fe flux, 100 μmol/m^2/yr in the Atlantic and
473 300 μmol/m^2/yr in the Pacific (Tagliabue et al., 2010). In one sense, this finding offers support for the
474 idea that the hydrothermal Fe flux from the Atlantic mid-ocean ridge is higher than would be expected
475 based on its relatively slow spreading rate (Saito et al., 2013). On the other hand, the observation that
476 dissolved Fe is transported in the deep ocean 4000 km away from a large source in the East Pacific Rise
477 (Fitzsimmons et al., 2014; Resing et al., 2015) suggests that the hydrothermal Fe must remain in the deep
478 ocean longer than a few years. However, this behavior may be ridge- or even vent-specific, depending on
479 ambient conditions and vent chemistry, such as the presence of H_2S.

480 One explanation for the persistence of Fe in deep water in the Pacific invokes stabilization by
481 colloids and/or ligands (Fitzsimmons et al., 2017, 2016) which may also have an origin in the

hydrothermal plumes, and which may not apply to lithogenic Fe from other sources. Thus, if Fe speciation or organic ligands are contributing to an apparently longer residence time in the plume measured in the GA03 section, the estimated hydrothermal Fe flux would not be as drastically high as calculated above. When Th and Fe data from the GEOTRACES program become available for other mid-ocean ridges in the Pacific, Arctic and Indian Oceans, we may gain more insight into how apparent anomalies in Th-supply-based Fe replacement times can be used to constrain hydrothermal Fe fluxes.

Similarly, the Th-based dissolved Mn flux is roughly 125 μmol/m^2/yr at the deep ridge site, while the Th-based replacement time there is 40 years (Fig. 6) rather than the 5 year replacement time of the basin-wide average (Fig. 7), implying a factor of 8 increased Mn flux (an additional 875 μmol/m^2/yr Mn flux from hydrothermal sources) to bring the replacement time estimate in line with the deep ocean average. Current estimates put the hydrothermal Mn flux at 10–20 μmol/m^2/yr along the ridge (van Hulten et al., 2017). Thus, either the Th-based replacement times imply a much higher hydrothermal Mn flux than is currently assumed, or again perhaps the residence time of Mn increases in the deep ocean near ridges due to stabilizing ligands of hydrothermal origin (Sander and Koschinsky, 2011), similar to Fe.

The millennial-scale replacement time of dissolved Zn estimated here (1100 ± 600 yrs) is short compared to the most recent residence estimates, 3,000–11,000 yrs (Bruland et al., 1994; Little et al., 2016; Roshan et al., 2016), but at least similar in order of magnitude, given the uncertainties involved. Additionally, Zn concentrations increase in the deep ocean along the conveyor circulation from the North Atlantic to the North Pacific by about a factor of 5 (Bruland et al., 2014). Thus, if calculated with a given Zn supply, one would expect a replacement time estimate to increase from the North Atlantic to the North Pacific or global ocean. Interestingly, the mid-ocean ridge does not appear to be a great source of Zn in the Atlantic (Roshan and Wu, 2015a), but it does in the Pacific and has been hypothesized to be an important global source (Roshan et al., 2016). This Zn source would clearly not be accounted for by Th supply, but this would mean our ~1,000 year replacement time estimate would overestimate the residence time due to not including a hydrothermal flux.

The other bioactive elements largely supplied by rivers, Cd and Cu, yielded replacement time estimates similar to previous estimates (Table 2) (Bruland et al., 1994; Little et al., 2017, 2015), though the estimates here have large uncertainties related to composition and solubility assumptions. For instance, using UCC composition and HAc leach solubility, the deep ocean replacement time of dissolved Cd averages 180,000 years (Fig. 6), but if we use North African dust composition and DI leach solubility, this estimate drops by 2 orders of magnitude to 1,800 years. As mentioned above, because the North African dust end-member may be contaminated by anthropogenic Cd, we take the average of the two possible estimates using the UCC composition (with DI leach and HAc leach) for the average North Atlantic Cd replacement time (180,000 and 33,000 years, average and standard deviation being 106,000 ± 103,000 years). This large uncertainty highlights the difficulty presented by predicting the replacement time of a mostly river-supplied element like Cd with a mostly dust-supplied element like Th.

In the case of Cu, uncertainty in both composition and solubility ratio lead to a fairly large range in replacement time estimates (5,200 ± 1400 years) with little reason to discount any of the parameters used. The geographical structure of the replacement time estimates (Figure 6) of Zn, Cd, and Cu is similar to those of the REEs, yielding increasing replacement times in the deep eastern Atlantic basin. It is likely that all of these elements have some supply from AABW into the North Atlantic (Conway and John, 2015, 2014b; Jacquot and Moffett, 2015; Roshan and Wu, 2015a, 2015b; Wu and Roshan, 2015). While the assumption of Th supply being a good analogue for the supply of other elements may be appropriate for some elements, it seems most tenuous for Zn, Cd and Cu. Nonetheless, our results at least agree with previous assessments that these elements have residence times similar to or longer than the timescale of ocean mixing (~1000 years).

5. Conclusion

Extrapolating the Th cycle to other elements in the periodic table has proved useful in assessing the range of trace element reactivity exhibited along the GA03 section in the North Atlantic and has potential applicability to the global ocean. Proof of concept for this method is demonstrated from Th-

based replacement times of the rare earth elements that follow known patterns of scavenging intensity. Among the bioactive elements, the evidence presented here suggests that the dissolved Fe residence time in the North Atlantic is decadal rather than centennial, and Fe and Mn may have the shortest residence times of all the elements in the ocean. Our Th-derived replacement time estimates for Zn, Cd, Cu, Co and Al largely agree with the best available estimates. Chief among the uncertainties associated with Th-based replacement times for the bioactive elements is how to define an appropriate source composition and relative solubility. Alternatively, if input ratios of specific sources (e.g., groundwater, modified estuarine water, or anthropogenically-contaminated water) could be better defined, a more complete assessment of trace element sources can be defined. The relatively simple Th-based replacement time method presented here can inform biogeochemical modelling of all trace elements and may be particularly useful for constraining the extremely rapidly cycled bioactive elements, Fe and Mn.

Acknowledgements

This study grew out of a synthesis workshop at the Lamont-Doherty Earth Observatory of Columbia University in August 2016, with financial support from the GEOTRACES Project Office (US NSF 1536294) and the Ocean Carbon and Biogeochemistry Program. The U.S. National Science Foundation supported all of the analytical work on GA03: Th isotope work at Columbia University, the University of Minnesota and the Woods Hole Oceanographic Institution (NSF OCE-0927064, -0926860, and -0927754); REE work at the University of Southern Mississippi (NSF OCE-0927951); and aerosol work at Florida State University (NSF OCE-0752832, -0929919 and -1132766). A portion of this work was performed at the National High Magnetic Field Laboratory, which is supported by National Science Foundation Cooperative Agreement No. DMR-1157490 and the State of Florida. The lead author acknowledges support from a start-up grant from the University of Southern Mississippi. This manuscript benefited from comments made by participants at the 2017 Gordon Research Conference on Chemical Oceanography at Colby-Sawyer College. GA03 data used in this study are accessible through the Biological and Chemical Oceanography Data Management Office (http://data.bco-dmo.org/jg/dir/BCO/GEOTRACES/NorthAtlanticTransect/). Basin-averaged North Atlantic data are available in the Supporting Information.

Figure and Table Captions

Figure 1. (Top) Dissolved ^{232}Th distribution along the east-west transect of GA03. (Middle) The stable isotopic composition of dissolved Fe (δ^{56}Fe) (Conway and John, 2014). Note the inverted scale on isotopic values. (Bottom) The dissolved ^{232}Th flux as a function of integration depth. The inset map on the bottom right shows the GA03 cruise tracks (blue) and the section plotted here (red).

Figure 2. Replacement times of dissolved REEs (Y, La, Nd, Sm, Eu, Gd, Dy, Ho, Er, Yb and La shown here; Pr, Tb and Tm not shown for brevity) as a function of integrated depth across the GA03 transect (small inset map). These replacement times are calculated with respect to supply based on dissolved

^{232}Th, assuming North African dust composition and HAc leach solubility ratios. The three plots in the top row are all on different colorbar scales. All plots in the bottom row use the same colorbar scale.

Figure 3. Average REE replacement times for the upper 1 km over the entire GA03 transect compared with ionic charge density of the same element. All elements were assumed to be trivalent cations, with the exception of Ce, for which the charge density of the tetravalent cation is shown. The grayscale curves represent the range of residence time estimates produced using different assumption for source material (upper continental crust, UCC, or North African aerosol samples, Dust) and relative fractional solubility of the REE to Th (defined using either a deionized water, DI, leach or a mild acetic acid solution, HAc, leach of North African dust aerosol samples).

Figure 4. Rare earth element ocean replacement times based on Th supply, averaged for the whole North Atlantic Basin in this study versus the residence times estimated by Li (1991) based on removal by sedimentation. The y-axis error bars reflect uncertainty in the REE/Th composition of source material and the relative solubility ratio. The dotted line is the 1-to-1 line.

Figure 5. Replacement times for the bioactive elements from this study (whole North Atlantic average) compared with the best available residence time estimates from previous studies. The error bars on the GA03 data represent uncertainty associated with crustal composition and solubility. The dotted line at 1000 years represents roughly the division of elements whose residence time is longer (Zn, Cu, Cd) or shorter (Fe, Mn, Al, Co) than the mixing time of the ocean.

Figure 6. Replacement times of dissolved Fe, Zn, Mn, Cd, Cu, Co and Al with respect to supply based on dissolved ^{232}Th input, assumed composition of the upper continental crust (Rudnick and Gao, 2014) and solubility ratios defined by mild acetic acid leaches of GA03 North African aerosols. The range in deep ocean (4 km) residence time estimates for these elements reported in Table 2 reflect uncertainty in source composition and solubility.

Figure 7. Trace element replacement times with respect to supply based on ^{232}Th supply. These profiles represent replacement times as a function of integration depth. To make a basin-wide average, the GA03 station profiles were averaged in depth bins on an area-weighted basis. The error bars represent the uncertainty in values used for the composition of the source (UCC or Saharan dust) and the relative solubility ratio (DI leach or HAc leach). For Mn, Zn and Cu, the solubility ratio defined by the HAc leach was used as the relative solubility from the DI leach for these elements was highly uncertain (see Table 2). Note that the Cd error bars nearly overlap with zero.

Table 1. REE/Th ratios of the average upper continental crust (Rudnick and Gao, 2014) and North African dust (Shelley et al., 2015), and deep ocean residence time estimates made here (see Sec. 3.3, and Eqs. 1–4) compared with whole ocean residence times based on deep sea sedimentation removal (Li, 1991). The fractional solubility ratios (S_{REE}/S_{Th}) are derived from leaching experiments of North African dust aerosols collected on GA03 using either deionized water (DI) or a weak acetic acid-type leach (HAc). Note that only 2 significant figures are shown here for brevity, but at least 3 significant figures were used in calculations.

Table 2. Upper continental crustal elemental ratios, relative solubility based on leaching experiments of North African dust aerosols from GA03, using a deionized water (DI) or a weak acetic acid-type leach (HAc), deep ocean (4 km) residence times based on this study (see Sec. 3.4 and Eqs. 1–4), and other published estimates of deep ocean residence times. Residence time estimates are denoted by the flux with respect to (w.r.t.) which they are based. Values are limited to a maximum of 3 significant figures here.

References

611 Aller, J.Y., Aller, R.C., 1986. Evidence for localized enhancement of biological activity associated with
612 tube and burrow structures in deep-sea sediments at the HEBBLE site, western North Atlantic. Deep
613 Sea Res. 33, 755–790. doi:10.1016/0198-0149(86)90088-9

614 Anderson, R.F., Cheng, H., Edwards, R.L., Fleisher, M.Q., Hayes, C.T., Huang, K., Kadko, D., Lam, P.J.,
615 Landing, W.M., Lao, Y., Lu, Y., 2016. How well can we quantify dust deposition to the ocean?
616 Philos. Trans. R. Soc. A 374, 20150285. doi:10.1098/rsta.2015.0285

617 Andersson, P.S., Wasserburg, G.J., Chen, J.H., Papanastassiu, D.A., Ingri, J., 1995. ^{238}U-^{234}U and ^{232}Th-
618 ^{230}Th in the Baltic Sea and in river water. Earth Planet. Sci. Lett. 130, 217–234. doi:10.1016/0012-
619 821X(94)00262-W

620 Arraes-Mescoff, R., Roy-Barman, M., Coppola, L., Souhaut, M., Tachikawa, K., Jeandel, C., Sempere,
621 R., Yoro, C., 2001. The behavior of Al, Mn, Ba, Sr, REE and Th isotopes during in vitro
622 degradation of large marine particles. Mar. Chem. 73, 1–19. doi:10.1016/S0304-4203(00)00065-7

623 Bacon, M.P., Anderson, R.F., 1982. Distribution of thorium isotopes between dissolved and particulate
624 forms in the deep sea. J. Geophys. Res. 87, 2045–2056. doi:10.1029/JC087iC03p02045

625 Barth, T.W., 1952. Theoretical Petrology. Wiley.

626 Berger, C.J.M., Lippiatt, S.M., Lawrence, M.G., Bruland, K.W., 2008. Application of a chemical leach
627 technique for estimating labile particulate aluminum, iron, and manganese in the Columbia River
628 plume and coastal waters off Oregon and Washington. J. Geophys. Res. 113, C00B01.
629 doi:10.1029/2007JC004703

630 Bergquist, B.A., Boyle, E.A., 2006. Dissolved iron in the tropical and subtropical Atlantic Ocean. Global
631 Biogeochem. Cycles 20, GB1015. doi:10.1029/2005GB002505

632 Berner, E.K., Berner, R.A., 2012. Global Environment: Water, Air and Geochemical Cycles, Second Edi.
633 ed. Princeton University Press, Princeton.

634 Bolin, B., Rodhe, H., 1973. A note on the concepts of age distribution and transit time in natural
635 reservoirs. Tellus 25, 58–62. doi:10.1111/j.2153-3490.1973.tb01594.x

636 Boyle, E.A., Edmond, J.M., Sholkovitz, E.R., 1977. The mechanism of iron removal in estuaries.
637 Geochim. Cosmochim. Acta 41, 1313–1324. doi:10.1016/0016-7037(77)90075-8

638 Broecker, W.S., 1971. A kinetic model for the chemical composition of sea water. Quat. Res. 1, 188–207.
639 doi:10.1016/0033-5894(71)90041-X

640 Bruland, K.W., Middag, R., Lohan, M.C., 2014. Controls of Trace Metals in Seawater, 2nd ed, The
641 Oceans and Marine Geochemistry. Elsevier Ltd. doi:10.1016/B978-0-08-095975-7.00602-1

642 Bruland, K.W., Orians, K.J., Cowen, J.P., 1994. Reactive trace metals in the stratified central North
643 Pacific. Geochim. Cosmochim. Acta 58, 3171–3182. doi:10.1016/0016-7037(94)90044-2

644 Buck, C.S., Landing, W.L., Resing, J.A., Lebon, G.T., 2006. Aerosol iron and aluminum solubility in the
645 northwest Pacific Ocean: Results from the 2002 IOC cruise. Geochemistry Geophys. Geosystems 7,
646 Q04M07. doi:10.1029/2005GC000977

647 Byrne, R., Kim, K.-H., 1990. Rare earth element scavenging in seawater. Geochim. Cosmochim. Acta 54,
648 2645–2656. doi:10.1016/0016-7037(90)90002-3

649 Censi, P., Zuddas, P., Randazzo, L.A., Saiano, F., Mazzola, S., Arico, P., Cuttitta, A., Punturo, R., 2010.
650 Influence of dissolved organic matter on rare earth elements and yttrium distributions in coastal
651 waters. Chem. Ecol. 26, 123–135. doi:10.1080/02757541003627720

Charette, M.A., Lam, P.J., Lohan, M.C., Kwon, E.Y., Hatje, V., Jeandel, C., Shiller, A.M., Cutter, G.A., Thomas, A., Boyd, P.W., Homocky, W.B., Milne, A., Thomas, H., Andersson, P.S., Porcelli, D., Tanaka, T., Geibert, W., Dehairs, F., Garcia-Orellana, 2016. Coastal ocean and shelf-sea biogeochemical cycling of trace elements and isotopes: lessons learned from GEOTRACES. Philos. Trans. R. Soc. A 374, 20160076.

Chester, R., Jickells, T., 2012. Trace elements in the oceans, in: Marine Geochemistry. Blackwell Publishing Ltd, pp. 223–252. doi:10.1002/9781118349083

Conway, T.M., John, S.G., 2015. Biogeochemical cycling of cadmium isotopes along a high-resolution section through the North Atlantic Ocean. Geochim. Cosmochim. Acta 148, 269–283. doi:10.1016/j.gca.2014.09.032

Conway, T.M., John, S.G., 2014a. Quantification of dissolved iron sources to the North Atlantic Ocean. Nature. doi:10.1038/nature13482

Conway, T.M., John, S.G., 2014b. The biogeochemical cycling of zinc and zinc isotopes in the North Atlantic Ocean. Global Biogeochem. Cycles 28, 1111–1128. doi:10.1002/2014GB004862

Elderfield, H., 1988. The oceanic chemistry of the rare-earth elements. Philos. Trans. R. Soc. A 325, 105–126. doi:10.1098/rsta.1988.0046

Fitzsimmons, J.N., Boyle, E.A., Jenkins, W.J., 2014. Distal transport of dissolved hydrothermal iron in the deep South Pacific Ocean. Proc. Natl. Acad. Sci. USA 111, 16654–16661. doi:10.1073/pnas.1418778111

Fitzsimmons, J.N., Conway, T.M., Lee, J.-M., Kayser, R., Thyng, K.M., John, S.G., Boyle, E.A., 2016. Dissolved iron and iron isotopes in the southeastern Pacific Ocean. Global Biogeochem. Cycles 30, 1372–1395. doi:10.1002/2015GB005357

Fitzsimmons, J.N., John, S.G., Marsay, C.M., Hoffman, C.L., Nicholas, S.L., Toner, B.M., German, C.R., Sherrell, R.M., 2017. Iron persistence in a distal hydrothermal plume supported by dissolved-particulate exchange. Nat. Geosci. 10, 195–201. doi:10.1038/NGEO2900

Gaillardet, J., Viers, J., Dupre, B., 2014. Trace Elements in River Waters, in: Holland, H.D., Turekian, K.K. (Eds.), Treatise on Geochemistry (Second Edition). Elsevier, Oxford, UK, doi: 10.1016/B978-0-08-095975-7.00507-6, pp. 195–235. doi:10.1016/B978-0-08-095975-7.00507-6

Grasse, P., Bosse, L., Hathorne, E.C., Böning, P., Pahnke, K., Frank, M., 2017. Short-term variability of dissolved rare earth elements and neodymium isotopes in the entire water column of the Panama Basin. Earth Planet. Sci. Lett. 475, 242–253. doi:10.1016/j.epsl.2017.07.022

Grousset, F.E., Quetel, C.R., Thomas, B., Donard, O.F.X., Lambert, C.E., Guillard, F., Monaco, A., 1995. Anthropogenic vs. lithogenic origins of trace elements (As, Cd, Pb, Rb, Sb, Sc, Sn, Zn) in water column particles: northwestern Mediterranean Sea. Mar. Chem. 48, 291–310. doi:10.1016/0304-4203(94)00056-J

Guo, L., Santschi, P.H., Baskaran, M., Zindler, A., 1995. Distribution of dissolved and particulate ^{230}Th and ^{232}Th in seawater from the Gulf of Mexico and off Cape Hatteras as measured by SIMS. Earth Planet. Sci. Lett. 133, 117–128.

Hatta, M., Measures, C.I., Wu, J., Roshan, S., Fitzsimmons, J.N., Sedwick, P., Morton, P., 2015. An overview of dissolved Fe and Mn distributions during the 2010 – 2011 U . S . GEOTRACES north Atlantic cruises : GEOTRACES GA03. Deep Sea Res. II 116, 117–129. doi:10.1016/j.dsr2.2014.07.005

694 Hawco, N.J., Lam, P.J., Lee, J., Daniel, C., Noble, A.E., Wyatt, N.J., Lohan, M.C., Saito, A., 2017.
695 Cobalt scavenging in the mesopelagic ocean and its influence on global mass balance: synthesizing
696 water column and sedimentary fluxes. Mar. Chem. in press. doi:10.1016/j.marchem.2017.09.001

697 Hayes, C.T., Anderson, R.F., Fleisher, M.Q., Huang, K.F., Robinson, L.F., Lu, Y., Cheng, H., Edwards,
698 R.L., Moran, S.B., 2015a. ^{230}Th and ^{231}Pa on GEOTRACES GA03, the U.S. GEOTRACES North
699 Atlantic transect, and implications for modern and paleoceanographic chemical fluxes. Deep Sea
700 Res. II 116, 29–41. doi:10.1016/j.dsr2.2014.07.007

701 Hayes, C.T., Anderson, R.F., Fleisher, M.Q., Serno, S., Winckler, G., Gersonde, R., 2013. Quantifying
702 lithogenic inputs to the North Pacific Ocean using the long-lived thorium isotopes. Earth Planet. Sci.
703 Lett. 383, 16–25. doi:10.1016/j.epsl.2013.09.025

704 Hayes, C.T., Fitzsimmons, J.N., Boyle, E.A., McGee, D., Anderson, R.F., Weisend, R., Morton, P.L.,
705 2015b. Thorium isotopes tracing the iron cycle at the Hawaii Ocean Time-series Station ALOHA.
706 Geochim. Cosmochim. Acta 169, 1–16. doi:10.1016/j.gca.2015.07.019

707 Hayes, C.T., Rosen, J., McGee, D., Boyle, E.A., 2017. Thorium distributions in high- and low-dust
708 regions and the significance for iron supply. Global Biogeochem. Cycles 31, 1–20.
709 doi:10.1002/2016GB005511

710 Henderson, G.M., Heinze, C., Anderson, R.F., Winguth, A.M.E., 1999. Global distribution of the 230Th
711 flux to ocean sediments constrained by GCM modelling. Deep Sea Res. I 46, 1861–1893.
712 doi:10.1016/S0967-0637(99)00030-8

713 Hirose, K., Sugimura, Y., 1987. Thorium Isotopes in the Surface Air of the Western North Pacific Ocean.
714 J. Environ. Radioact. 5, 459–475. doi:10.1016/0265-931X(87)90020-8

715 Hsieh, Y.-T., Henderson, G.M., Thomas, A.L., 2011. Combining seawater ^{232}Th and ^{230}Th concentrations
716 to determine dust fluxes to the surface ocean. Earth Planet. Sci. Lett. 312, 280–290.
717 doi:10.1016/j.epsl.2011.10.022

718 Huh, C.-A., Bacon, M.P., 1985. Thorium-232 in the eastern Caribbean Sea. Nature 316, 718–721.
719 doi:10.1038/316718a0

720 Jacquot, J.E., Moffett, J.W., 2015. Copper distribution and speciation across the International
721 GEOTRACES Section GA03. Deep Sea Res. II 116, 187–207. doi:10.1016/j.dsr2.2014.11.013

722 Jenkins, W.J., Jr, W.M.S., Boyle, E.A., Cutter, G.A., 2015a. Deep-Sea Research II Water mass analysis
723 for the U . S . GEOTRACES (GA03) North Atlantic sections. Deep. Res. Part II 116, 6–20.
724 doi:10.1016/j.dsr2.2014.11.018

725 Jenkins, W.J., Lott, D.E., Longworth, B.E., Curtice, J.M., Cahill, K.L., 2015b. The distributions of helium
726 isotopes and tritium along the U.S. GEOTRACES North Atlantic sections (GEOTRACES GAO3).
727 Deep Sea Res. II 116, 21–28. doi:10.1016/j.dsr2.2014.11.017

728 John, S.G., Adkins, J., 2012. The vertical distribution of iron stable isotopes in the North Atlantic near
729 Bermuda. Global Biogeochem. Cycles 26, 1–10. doi:10.1029/2011GB004043

730 Kipp, L.E., Sanial, V., Henderson, P.B., van Beek, P., Reyss, J.-L., Hammond, D.E., Moore, W.S.,
731 Charette, M.A., 2017. Radium isotopes as tracers of hydrothermal inputs and neutrally buoyant
732 plume dynamics in the deep ocean. Mar. Chem. in press. doi:10.1016/j.marchem.2017.06.011

733 Kulaksiz, S., Bau, M., 2007. Contrasting behaviour of anthropogenic gadolinium and natural rare earth
734 elements in estuaries and the gadolinium input into the North Sea. Earth Planet. Sci. Lett. 260, 361–
735 371. doi:10.1016/j.epsl.2007.06.016

Lam, P.J., Ohnemus, D.C., Auro, M.E., 2015. Size-fractionated major particle composition and concentrations from the US GEOTRACES North Atlantic Zonal Transect. Deep Sea Res. II 116, 303–320. doi:10.1016/j.dsr2.2014.11.020

Li, Y.-H., 1991. Distribution patterns of the elements in the ocean: a synthesis. Geochim. Cosmochim. Acta 55, 3223–3240. doi:10.1016/0016-7037(91)90485-N

Little, S.H., Vance, D., Lyons, T.W., McManus, J., 2015. Controls on trace metal authigenic enrichment in reducing sediments: insights from modern oxygen-deficient settings. Am. J. Sci. 315, 77–119. doi:10.2475/02.2015.01

Little, S.H., Vance, D., McManus, J., Severmann, S., 2016. Key role of continental margin sediments in the oceanic mass balance of Zn and Zn isotopes. Geology 44, 1–4. doi:10.1130/G37493.1

Little, S.H., Vance, D., McManus, J., Severmann, S., Lyons, T.W., 2017. Copper isotope signatures in modern marine sediments. Geochim. Cosmochim. Acta 212, 253–273. doi:10.1016/j.gca.2017.06.019

Mawji, E., et al., 2015. The GEOTRACES Intermediate Data Product 2014. Mar. Chem. 177, 1–8.

Measures, C., Hatta, M., Fitzsimmons, J., Morton, P., 2015. Dissolved Al in the zonal N Atlantic section of the US GEOTRACES 2010/2011 cruises and the importance of hydrothermal inputs. Deep Sea Res. II 116, 176–186. doi:10.1016/j.dsr2.2014.07.006

Middag, R., Hulten, M.M.P. Van, Aken, H.M. Van, Rijkenberg, M.J.A., Gerringa, L.J.A., Laan, P., Baar, H.J.W. De, 2015. Dissolved aluminium in the ocean conveyor of the West Atlantic Ocean : Effects of the biological cycle , scavenging , sediment resuspension and hydrography. Mar. Chem. 177, 69–86. doi:10.1016/j.marchem.2015.02.015

Moran, S.B., Moore, R.M., 1989. The distribution of colloidal aluminum and organic carbon in coastal and open ocean waters off Nova Scotia. Geochim. Cosmochimca Acta 53, 2519–2527. doi:10.1016/0016-7037(89)90125-7

Morel, F.M.M., Price, N.M., 2003. The Biogeochemical Cycles of Trace Metals. Science 300, 944–947. doi:10.1126/science.1083545

Morton, P.L., Landing, W.M., Hsu, S., Milne, A., Aguilar-islas, A.M., Baker, A.R., Bowie, A.R., 2013. Methods for the sampling and analysis of marine aerosols: results from the 2008 GEOTRACES aerosol intercalibration experiment. Limnol. Oceanogr. Methods 11, 62–78. doi:10.4319/lom.2013.11.62

Noble, A.E., Ohnemus, D.C., Hawco, N.J., Lam, P.J., Saito, M.A., 2017. Coastal sources, sinks and strong organic complexation of dissolved cobalt within the US North Atlantic GEOTRACES Transect GA03. Biogeosciences 14, 2715–2739. doi:10.5194/bg-2016-512

Pavia, F., Anderson, R., Vivancos, S., Fleisher, M., Lam, P., Lu, Y., Cheng, H., Zhang, P., Edwards, R.L., 2017. Intense hydrothermal scavenging of ^{230}Th and ^{231}Pa in the deep Southeast Pacific. Mar. Chem. in press. doi:10.1016/j.marchem.2017.08.003

Quinn, K.A., Byrne, R., Schijf, J., 2004. Comparative scavenging of yttrium and the rare earth elements in seawater: Competitive influences of solution and surface chemistry. Aquat. Geochemistry 10, 59–80. doi:10.1023/B:AQUA.0000038959.03886.60

Rayner-Canham, G., Overton, T., 2006. Descriptive Inorgranic Chemistry, 4th ed. W. H. Freeman, New York.

Resing, J.A., Sedwick, P.N., German, C.R., Jenkins, W.J., Moffett, J.W., Sohst, B.M., Tagliabue, A., 2015. Basin-scale transport of hydrothermal dissolved metals across the South Pacific Ocean. Nature 523, 200–203. doi:10.1038/nature14577

Robinson, L.F., Noble, T.L., McManus, J.F., 2008. Measurement of adsorbed and total $^{232}Th/^{230}Th$ ratios from marine sediments. Chem. Geol. 252, 169–179. doi:10.1016/j.chemgeo.2008.02.015

Roshan, S., Wu, J., 2015a. Water mass mixing: the dominant control on the zinc distribution in the North Atlantic Ocean. Global Biogeochem. Cycles 29, 1060–1074. doi:10.1002/2014GB005026

Roshan, S., Wu, J., 2015b. The distribution of dissolved copper in the tropical-subtropical north Atlantic across the GEOTRACES GA03 transect. Mar. Chem. 176, 189–198. doi:10.1016/j.marchem.2015.09.006

Roshan, S., Wu, J., Jenkins, W.J., 2016. Long-range transport of hydrothermal dissolved Zn in the tropical South Pacific. Mar. Chem. 183, 25–32. doi:10.1016/j.marchem.2016.05.005

Rowland, G.H., Ng, H.C., Robinson, L.F., Mcmanus, J.F., Mohamed, K.J., Mcgee, D., 2017. Investigating the use of $^{232}Th/^{230}Th$ as a dust proxy using co-located seawater and sediment samples from the low-latitude North Atlantic. Geochim. Cosmochim. Acta in press. doi:10.1016/j.gca.2017.07.033

Roy-Barman, M., Coppola, L., Souhaut, M., 2002. Thorium isotopes in the western Mediterranean Sea: an insight into the marine particle dynamics. Earth Planet. Sci. Lett. 196, 161–174. doi:10.1016/S0012-821X(01)00606-9

Rudnick, R.L., Gao, S., 2014. Composition of the Continental Crust, in: Holland, H.D., Turekian, K.K. (Eds.), Treatise on Geochemistry (Second Edition). Elsevier, Oxford, UK, doi: 10.1016/B978-0-08-095975-7.00301-6, pp. 1–51. doi:10.1016/B978-0-08-095975-7.00301-6

Saito, M.A., Moffett, J.W., 2002. Temporal and spatial variability of cobalt in the Atlantic Ocean. Geochim. Cosmochim. Acta 66, 1943–1953. doi:10.1016/S0016-7037(02)00829-3

Saito, M.A., Noble, A.E., Tagliabue, A., Goepfert, T.J., Lamborg, C.H., Jenkins, W.J., 2013. Slow-spreading submarine ridges in the South Atlantic as a significant oceanic iron source. Nat. Geosci. 6, 775–779. doi:10.1038/ngeo1893

Sander, S.G., Koschinsky, A., 2011. Metal flux from hydrothermal vents increased by organic complexation. Nat. Geosci. 4, 145–150. doi:10.1038/ngeo1088

Schijf, J., Christenson, E.A., Byrne, R.H., 2015. YREE scavenging in seawater: A new look at an old model. Mar. Chem. 177, 460–471. doi:10.1016/j.marchem.2015.06.010

Severmann, S., Johnson, C.M., Beard, B.L., Mcmanus, J., 2006. The effect of early diagenesis on the Fe isotope compositions of porewaters and authigenic minerals in continental margin sediments. Geochim. Cosmochim. Acta 70, 2006–2022. doi:10.1016/j.gca.2006.01.007

Shelley, R.U., Landing, W.M., Ussher, S.J., Planquett, H., Sarthou, G., 2018. Characterisation of aerosol provenance from the fractional solubility of Fe (Al, Ti, Mn, Co, Ni, Cu, Zn, Cd and Pb) in North Atlantic aerosols (GEOTRACES GA01 and GA03). Biogeosciences 1–31. doi:10.5194/bg-2017-415

Shelley, R.U., Morton, P.L., Landing, W.M., 2015. Elemental ratios and enrichment factors in aerosols from the US-GEOTRACES North Atlantic transects. Deep Sea Res. II 116, 262–272. doi:10.1016/j.dsr2.2014.12.005

Shiller, A.M., 2016a. Dissolved rare earth element (REE) concentrations from the GEOTRACES North

Atlantic Transect (Section GA03) collected on the R/V Knorr KN199-04, KN199-05, KN204-01 during 2010 (U.S. GEOTRACES NAT project). Biol. Chem. Oceanogr. Data Manag. Off. doi:http://lod.bco-dmo.org/id/dataset/651138

Shiller, A.M., 2016b. Dissolved Rare Earth Elements in the US GEOTRACES North Atlantic Section. Goldschmidt Abstr. 2827.

Shiller, A.M., 1997. Dissolved trace elements in the Mississippi River: seasonal, interannual, and decadal variability. Geochim Cosmochim Acta 61, 4321–4330. doi:10.1016/S0016-7037(97)00245-7

Stichel, T., Hartman, A.E., Duggan, B., Goldstein, S.L., Scher, H., Pahnke, K., 2015. Separating biogeochemical cycling of neodymium from water mass mixing in the Eastern North Atlantic. Earth Planet. Sci. Lett. 412, 245–260. doi:10.1016/j.epsl.2014.12.008

Stichel, T., Pahnke, K., Duggan, B., Goldstein, S.L., Hartman, A.E., Paffrath, R., Scher, H.D., 2018. TAG Plume: Revisiting the Hydrothermal Neodymium Contribution to Seawater. Front. Mar. Sci. 5, 1–11. doi:10.3389/fmars.2018.00096

Tachikawa, K., Arsouze, T., Bayon, G., Colin, C., Dutay, J.-C., Frank, N., Giraud, X., Gourlan, A.T., Jeandel, C., Meynadier, L., Montagna, P., Alexander, M., Plancherel, Y., Pucéat, E., Roy-, M., Waelbroeck, C., Gourlan, T., Jeandel, C., Lacan, F., Meynadier, L., Montagna, P., 2017. The large-scale evolution of neodymium isotopic composition in the global modern and Holocene ocean revealed from seawater and archiva data. Chem. Geol. 457, 131–148. doi:10.1016/j.chemgeo.2017.03.018

Tachikawa, K., Jeandel, C., Roy-Barman, M., 1999. A new approach to the Nd residence time in the ocean : the role of atmospheric inputs. Earth Planet. Sci. Lett. 170, 433–446. doi:10.1016/S0012-821X(99)00127-2

Tagliabue, A., Aumont, O., Bopp, L., 2014. The impact of different external sources of iron on the global carbon cycle. Geophys. Res. Lett. 41, 920–926. doi:10.1002/2013GL059059.Received

Tagliabue, A., Aumont, O., DeAth, R., Dunne, J.P., Dutkiewicz, S., Galbraith, E., Misumi, K., Moore, J.K., Ridgewell, A., Sherman, E., Stock, C., Vichi, M., Volker, C., Yool, A., 2016. How well do global ocean biogeochemistry models simulate dissolved iron distributions? Global Biogeochem. Cycles 30, 149–174. doi:10.1016/S0074-6142(08)62690-X

Tagliabue, A., Bopp, L., Dutay, J., Bowie, A.R., Chever, F., Jean-baptiste, P., Bucciarelli, E., Lannuzel, D., Remenyi, T., Sarthou, G., Aumont, O., Gehlen, M., Jeandel, C., 2010. Hydrothermal contribution to the oceanic dissolved iron inventory. Nat. Geosci. 3, 252–256. doi:10.1038/ngeo818

Tagliabue, A., Bowie, A.R., Philip, W., Buck, K.N., Johnson, K.S., Saito, M.A., 2017. The integral role of iron in ocean biogeochemistry. Nature 543, 51–59. doi:10.1038/nature21058

van Hulten, M., Middag, R., Dutay, J., Baar, H. De, Roy-barman, M., Gehlen, M., Tagliabue, A., Sterl, A., Lsce, E., Orme, C.E.A., 2017. Manganese in the west Atlantic Ocean in the context of the first global ocean circulation model of manganese. Biogeosciences 14, 1123–1152. doi:10.5194/bg-14-1123-2017

Wu, J., Roshan, S., 2015. Cadmium in the North Atlantic: Implication for global cadmium-phosphorus relationship. Deep Sea Res. II 116, 226–239. doi:10.1016/j.dsr2.2014.11.007

Wu, J., Roshan, S., Chen, G., 2014. The distribution of dissolved manganese in the tropical-subtropical North Atlantic during US GEOTRACES 2010 and 2011 cruises. Mar. Chem. 166, 9–24. doi:10.1016/j.marchem.2014.08.007

Zheng, X., Plancherel, Y., Saito, M.A., Scott, P.M., Henderson, G.M., 2016. Rare earth elements (REEs) in the tropical South Atlantic and quantitative deconvolution of their non-conservative behavior. Geochim. Cosmochim. Acta 177, 217–237. doi:10.1016/j.gca.2016.01.018

Fig 1.

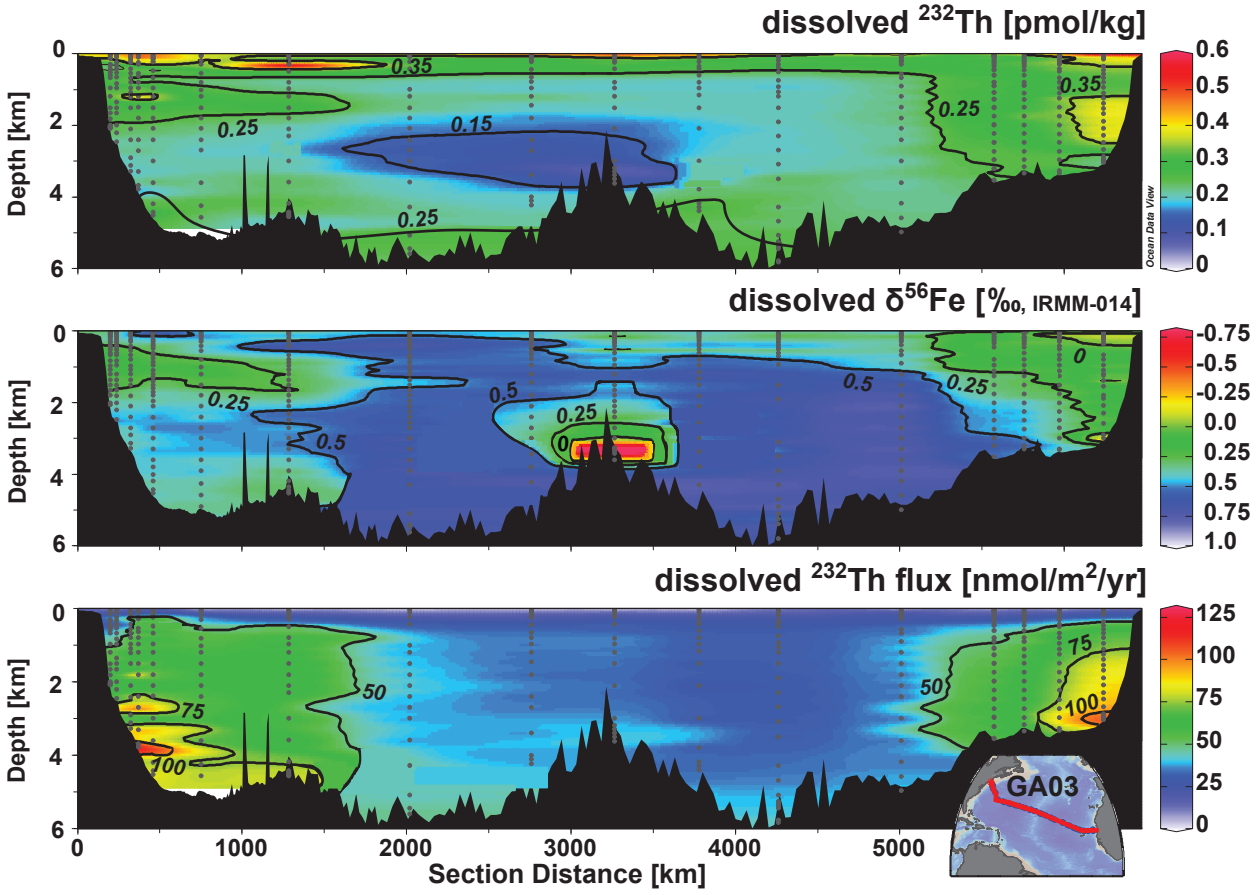
dissolved 232Th [pmol/kg]
Depth [km]
0
2
4
6
0.35
0.25
0.15
0.25
0.25
0.35
0.6
0.5
0.4
0.3
0.2
0.1
0
Ocean Data View
dissolved δ56Fe [‰, IRMM-014]
Depth [km]
0.25
0.5
0.5
0.25
0
0.5
0.25
0
-0.75
-0.5
-0.25
0.0
0.25
0.5
0.75
1.0
dissolved 232Th flux [nmol/m2/yr]
Depth [km]
75
50
50
75
100
100
125
100
75
50
25
0
GA03
0
1000
2000
3000
4000
5000
Section Distance [km]

Fig 2.

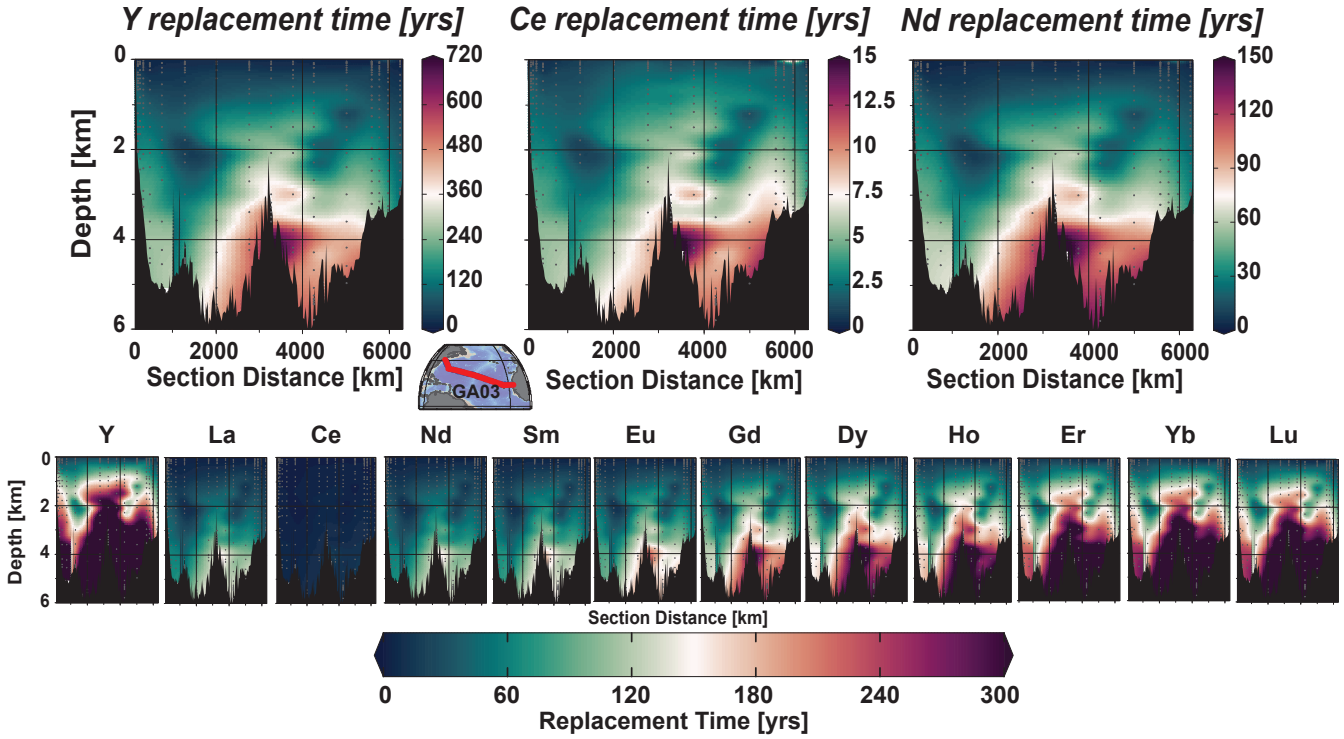
Y replacement time [yrs]
Ce replacement time [yrs]
Nd replacement time [yrs]
Depth [km]
0
2
4
6
0
2000
4000
6000
Section Distance [km]
720
600
480
360
240
120
0
15
12.5
10
7.5
5
2.5
150
120
90
60
30
GA03
Y
La
Ce
Nd
Sm
Eu
Gd
Dy
Ho
Er
Yb
Lu
0
60
120
180
240
300
Replacement Time [yrs]

Fig 3.

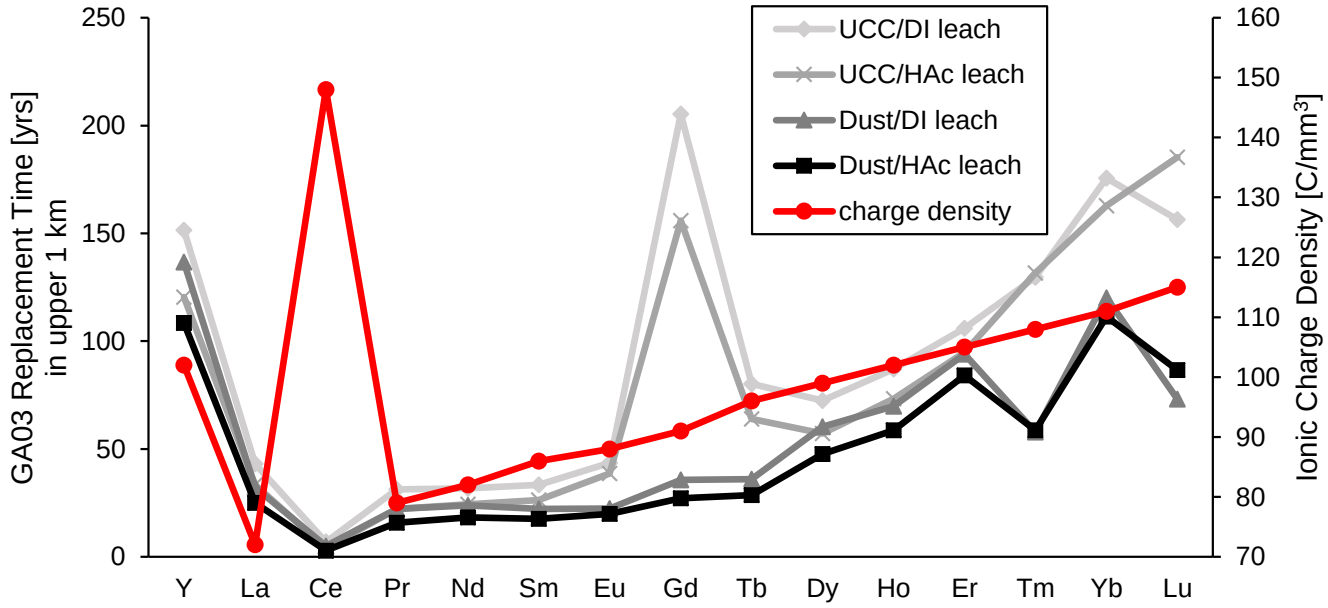
GA03 Replacement Time [yrs]
in upper 1 km
Ionic Charge Density [C/mm³]
250
200
150
100
50
0
160
150
140
130
120
110
100
90
80
70
Y
La
Ce
Pr
Nd
Sm
Eu
Gd
Tb
Dy
Ho
Er
Tm
Yb
Lu
UCC/DI leach
UCC/HAc leach
Dust/DI leach
Dust/HAc leach
charge density

Fig 4.

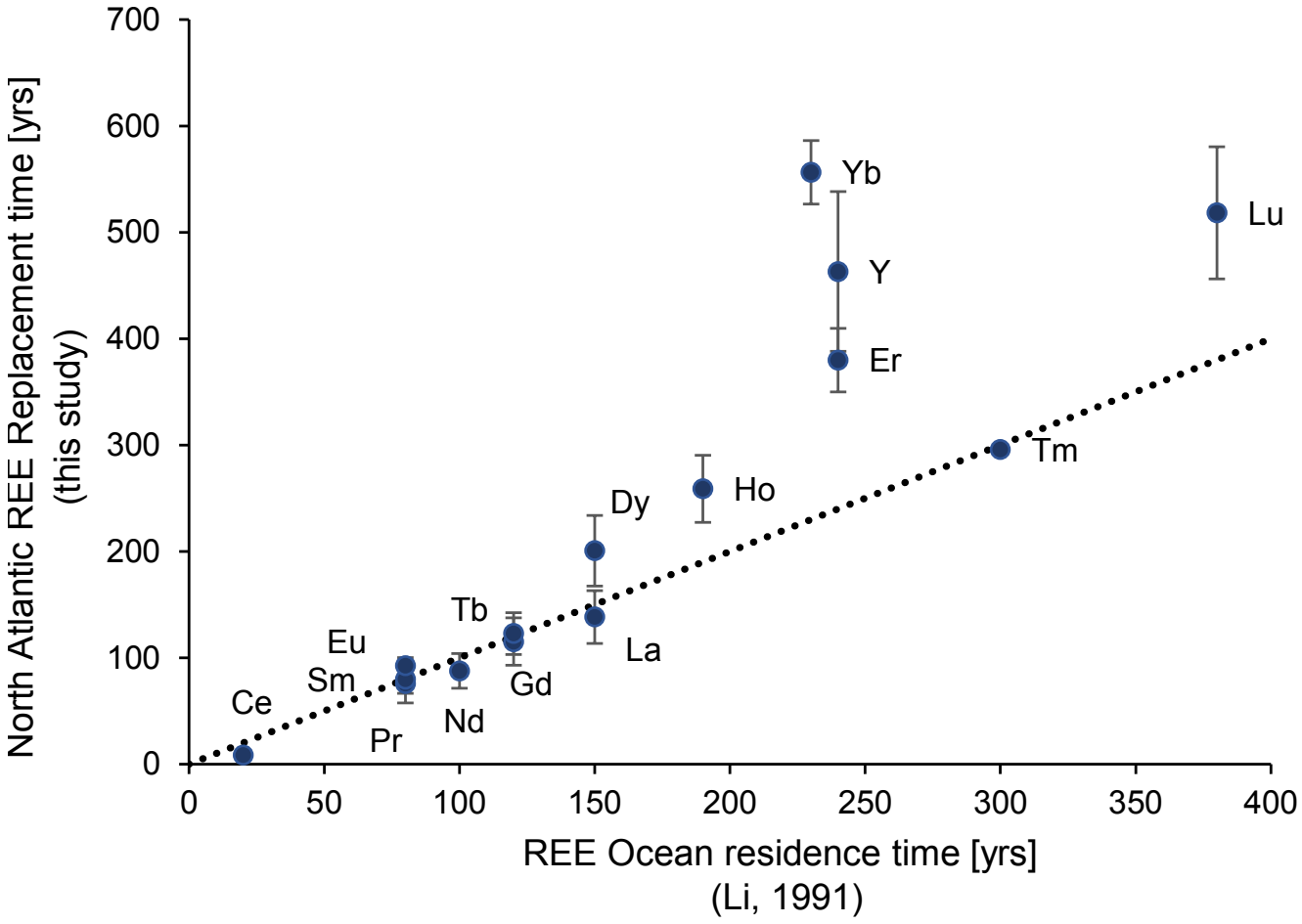
North Atlantic REE Replacement time [yrs]
(this study)
REE Ocean residence time [yrs]
(Li, 1991)
0
100
200
300
400
500
600
700
0
50
100
150
200
250
300
350
400
Ce
Pr
Nd
Sm
Eu
Gd
Tb
Dy
Ho
Er
Y
Yb
Lu
Tm
La

Fig 5.

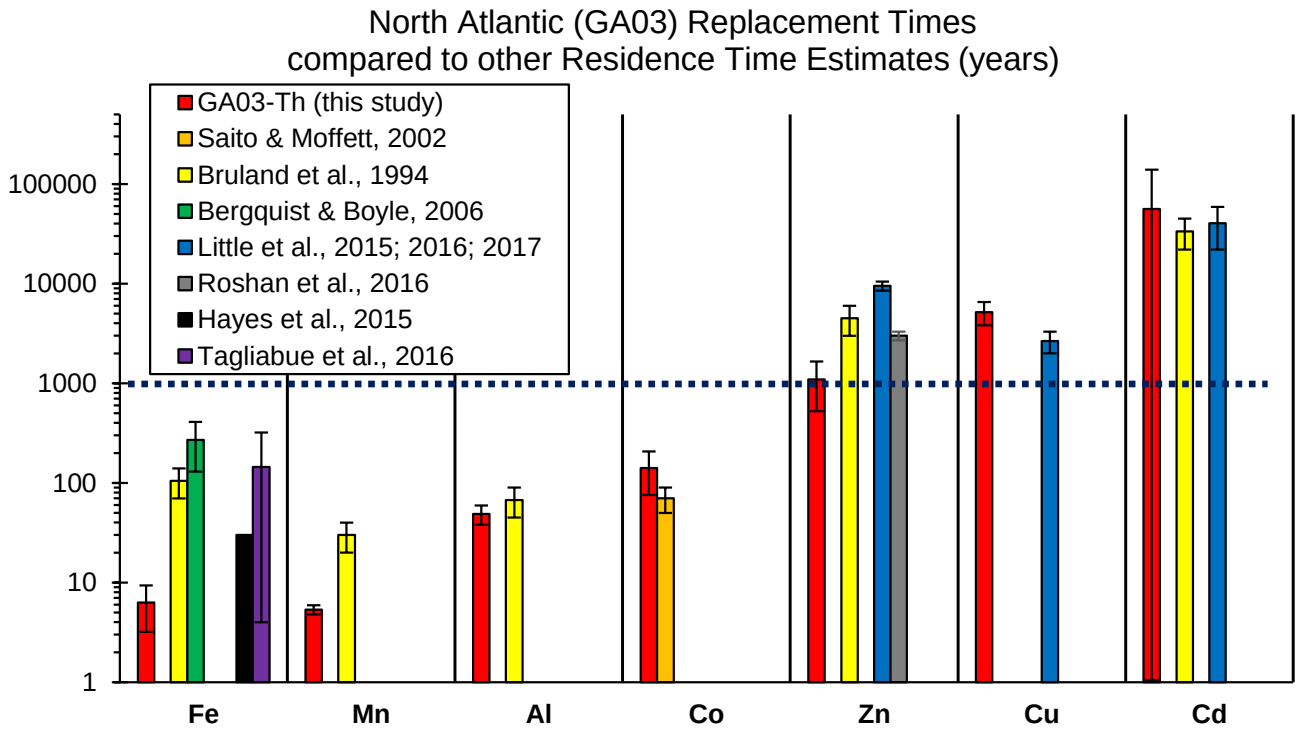
North Atlantic (GA03) Replacement Times
compared to other Residence Time Estimates (years)
GA03-Th (this study)
Saito & Moffett, 2002
Bruland et al., 1994
Bergquist & Boyle, 2006
Little et al., 2015; 2016; 2017
Roshan et al., 2016
Hayes et al., 2015
Tagliabue et al., 2016
100000
10000
1000
100
10
1
Fe
Mn
Al
Co
Zn
Cu
Cd

Fig 6.

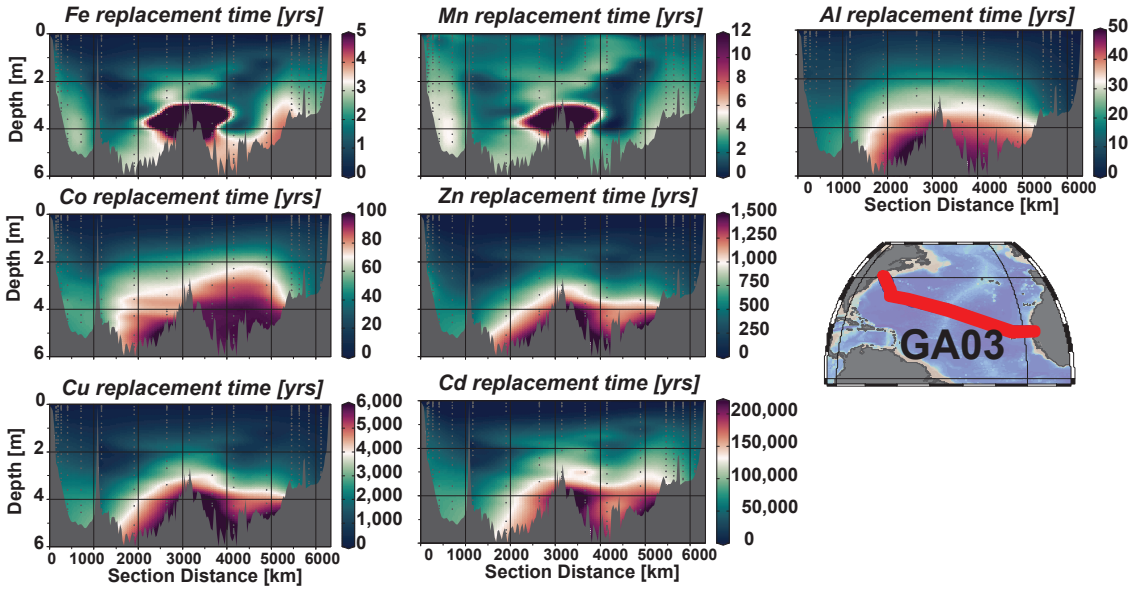
Fe replacement time [yrs]
Mn replacement time [yrs]
Al replacement time [yrs]
Co replacement time [yrs]
Zn replacement time [yrs]
Cu replacement time [yrs]
Cd replacement time [yrs]
Depth [m]
Section Distance [km]
GA03

Fig 7.

North Atlantic Replacement Times (GA03)

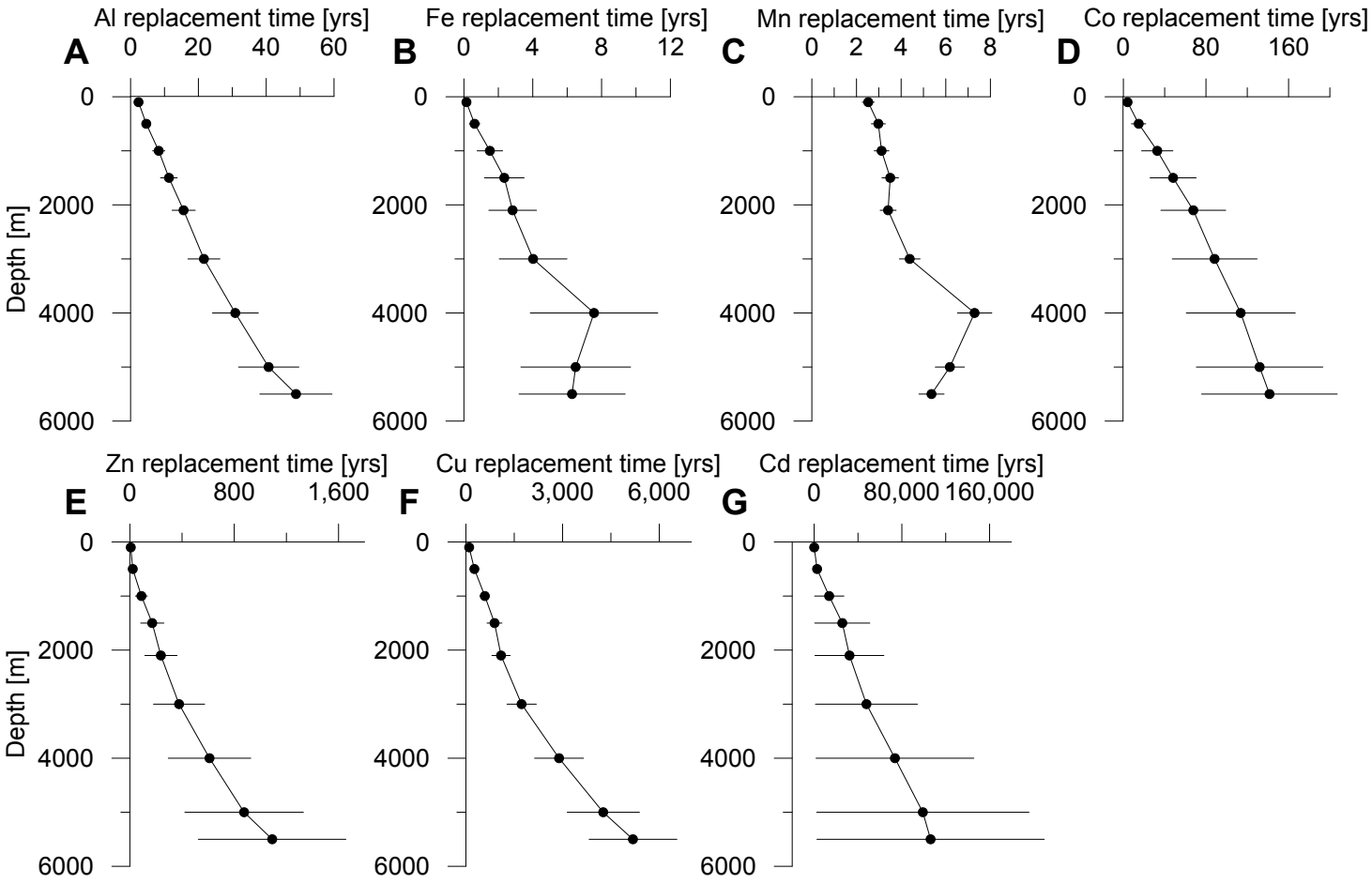

Table 1. REE/Th ratios of the average upper continental crust (Rudnick and Gao, 2014) and North African dust (Shelley et al., 2015), and deep ocean residence time estimates made here (see Sec. 3.3, and Eqs. 1–4) compared with whole ocean residence times based on deep sea sedimentation removal (Li, 1991). The fractional solubility ratios (S_{REE}/S_{Th}) are derived from leaching experiments of North African dust aerosols collected on GA03 using either deionized water (DI) or a weak acetic acid-type leach (HAc). Note that only 2 significant figures are shown here for brevity, but at least 3 significant figures were used in calculations.

REE:	**Y**	**La**	**Ce**	**Pr**	**Nd**	**Sm**	**Eu**	**Gd**	**Tb**	**Dy**	**Ho**	**Er**	**Tm**	**Yb**	**Lu**
REE/Th UCC [mol/mol]	5.2	4.9	9.9	1.1	4.1	0.69	0.15	0.56	0.10	0.53	0.11	0.30	0.039	0.25	0.039
REE/Th North African [mol/mol]	5.8	6.6	14	1.6	5.6	1.0	0.28	3.2	0.22	0.64	0.14	0.34	0.088	0.37	0.084
S_{REE}/S_{Th} DI leach	3.8	2.1	2.2	2.4	3.1	3.6	3.5	1.0	2.2	3.6	3.3	3.6	2.8	2.3	2.4
S_{REE}/S_{Th} HAc leach	4.8	2.7	3.8	3.4	4.1	4.5	3.9	1.4	2.7	4.5	3.8	4.0	2.8	2.5	2.1
North Atlantic replacement time [yrs]	580 ±90	180 ±30	15 ±6	110 ±30	110 ±20	100 ±20	100 ±10	150 ±30	150 ±30	250 ±40	310 ±40	420 ±30	290 ±3	600 ±30	440 ±50
Whole Ocean Residence Time (Li, 1991) [yrs]	240	150	20	80	100	80	80	120	120	150	190	240	300	230	380

Table 2. Upper continental crustal elemental ratios, relative solubility based on leaching experiments of North African dust aerosols from GA03, using a deionized water (DI) or a weak acetic acid-type leach (HAc), deep ocean (4 km) residence times based on this study (see Sec. 3.4 and Eqs. 1–4), and other published estimates of deep ocean residence times. Residence time estimates are denoted by the flux with respect to (w.r.t.) which they are based. Values are limited to a maximum of 3 significant figures here.

	Al	**Fe**	**Mn**	**Zn**	**Cd**	**Cu**	**Co**
$(Metal/Th)_{UCC}$ [mol/mol]	33,400	15,500	312	22.6	0.0177	9.74	6.49
Metal/Th North African dust [mol/mol]	41,600	15,700	268	48.8	0.326	14.2	6.49
Metal/Th Rivers [mol/mol] (Gaillardet et al., 2014)	6,710	6,690	3,500	51.9	4.03	132	14.2
S_{Metal}/S_{Th} DI leach	1.5±0.9 (n=12)	0.4±0.2 (n=2)	3841± 804 (n=2)	20±19 (n=2)	54±40 (n=12)	5.4±3.6 (n=12)	14±7 (n=12)
S_{Metal}/S_{Th} HAc leach	2.0±0.4 (n=7)	1.3±0.3 (n=7)	9.8±2.4 (n=7)	6.7±3.5 (n=7)	10.0±5.2 (n=7)	3.4±1.1 (n=7)	5.9±1.5 (n=7)
Deep North Atlantic replacement time w.r.t Th supply (GA03) [yrs]	50 ± 10	6 ± 3	5 ± 1	1,100 ±600	105,000 ±103,000	5,200 ±1,300	140±70
Other residence time estimates:							
Deep Pacific residence time w.r.t. deep water scavenging (Bruland et al., 1994) **[yrs]**	45–90	70–140	20–40	3,000–6,000	22,000–45,000		
Whole Ocean residence time from mass balances (Little et al., 2017, 2016, 2015) **[yrs]**				8,000–11,000	26,000–55,000	2,000–3,300	
Deep Atlantic residence time w.r.t. deep water scavenging (Bergquist and Boyle, 2006) **[yrs]**		130–410					
Deep Pacific (4 km) residence time w.r.t. Th supply (Hayes et al., 2015b) **[yrs]**		30					
Whole Ocean residence time from global ocean biogeochemistry models (Tagliabue et al., 2016) **[yrs]**		4–560					
Whole Ocean residence time [*Roshan et al., 2016*]				2,400–3,600			
Deep Atlantic residence time w.r.t deep sea sedimentation (Saito and Moffett, 2002) **[yrs]**							40–120

Global Biogeochemical Cycles

Supporting Information for

Replacement times of a spectrum of elements in the North Atlantic based on thorium supply

Christopher T. Hayes[1], Robert F. Anderson[2,3], H. Cheng[4,5], Tim M. Conway[6], R. Lawrence Edwards[5], M. Q. Fleisher[2], Peng Ho[1], Kuo-Fang Huang[7], Seth G. John[8], William M. Landing[9], Susan H. Little[10], Yanbin Lu[11], Peter L. Morton[9], S. Bradley Moran[12], Laura F. Robinson[13], Rachel U. Shelley[9], Alan M. Shiller[1], Xin-Yuan Zheng[14]

Contents of this file

[1] School of Ocean Science and Technology, University of Southern Mississippi, Stennis Space Center, MS, USA (Christopher.t.hayes@usm.edu)
[2] Lamont-Doherty Earth Observatory and Palisades, Columbia University, Palisades, NY, USA
[3] Department of Earth and Environmental Sciences, Columbia University, New York, NY, USA
[4] Institute of Global Environmental Change, Xi'an Jiaotong University, Xi'an, China
[5] Department of Earth Sciences, University of Minnesota, Minneapolis, MN, USA
[6] College of Marine Science, University of South Florida, St. Petersburg, FL, USA
[7] Institute of Earth Sciences, Academica Sinica, Taipei, Taiwan
[8] Department of Earth Sciences, University of Southern California, Los Angeles, CA, USA
[9] Department of Earth, Ocean and Atmospheric Science, Florida State University, Tallahassee, FL, USA
[10] Department of Earth Science and Engineering, Royal School of Mines, Imperial College London, London, UK
[11] Earth Observatory of Singapore, Singapore, Republic of Singapore
[12] College of Fisheries and Ocean Sciences, University of Alaska, Fairbanks, Alaska, USA
[13] Department of Earth Sciences, University of Bristol, Bristol, UK
[14] Department of Geoscience, University of Wisconsin, Madison, Wisconsin, USA

Supplementary Text

This file contains additional results of the replacement time calculations based on dissolved ^{232}Th flux for which space in the main text did not allow discussion. In Figure S1, we show how replacement time estimates were averaged to derive a basin-wide North Atlantic average. In Figure S2, the same replacement time estimates as plotted in Figure 7 of the main text (North Atlantic basin-wide averages), but zoomed in on the upper 1000 m, to examine the replacement time results in the environment of significant biological uptake. The shortest replacement time in the upper 100 m of the bioactive elements considered is Fe, about 1–2 months. This is roughly 5 times shorter than the same estimate made at the Hawaii Ocean Time series station (Hayes et al., 2015) in the North Pacific. This implies either: (1) very rapid biological removal since the input of Fe to the North Atlantic is much greater than in the North Pacific (Hayes et al., 2017) or (2) more efficient biological retention of Fe in the Fe-poor North Pacific (Rafter et al., 2017). Zinc, cobalt, and manganese all have dissolved replacement times less than 6 years in the upper 100 m, also indicating quite rapid turnover. Dissolved Al has a replacement time of about 2.3 ± 0.5 years in the upper 100 m, shorter than with the usual assumption of a 5 years residence time in the mixed layer (Measures and Brown, 1996). Copper and cadmium have much longer replacement times in the upper 100 m (80–90 years), perhaps surprisingly given their role as micronutrients. Of course, as discussed in the main text, there are large uncertainties with respect to source composition and relative solubility especially for these elements.

In figures S3 and S4, we show replacement time calculations for other elements of geochemical interest, for which data are available in the GA03 data product: Sc, V, Ni, Ga, and Ba. Sections plots are shown in Figure S3 and the North Atlantic averages in Figure S4. For these estimates we have used the assumption of upper continental crustal source (Rudnick and Gao, 2014) and any available data from the DI leaches (Shelley et al., 2018) (see Table S1). Based on enrichment factor analyses, North African dust is contaminated with anthropogenic V and Ni (Shelley et al., 2015; Trapp et al., 2010). This potentially leads the V/Th and Ni/Th solubility ratios (reported in Table S1) being elevated over natural inputs and thus may lead to our replacement time estimates for V and Ni being underestimates of the residence time. Available leach data for Sc and Ga was minimal, so we made a basic assumption of similar fractional solubility to Th for Sc ($S_{Sc}/S_{Th} = 1$) since this is a highly scavenged element (Parker et al., 2016) and greater solubility for Ga than Th ($S_{Ga}/S_{Th} = 5$) since this element is scavenged less intensely than Al (Shiller and Bairamadgi, 2006) and thus likely much less intensely than Th. Deep ocean estimates indicate Sc and Ga are relatively short-lived, with 5 km replacement times of about 160 years or less, and both elements may be good analogues for lithogenic, scavenged elements like thorium. Barium and nickel have intermediate length replacement times (5 km replacement times of about 5,000 years), which indicates their role in biological cycles. Consistent with the Th-based result, whole ocean Ba replacement time is estimated as about 10,000 years (Chan et al., 1976). The deep ocean replacement time of dissolved vanadium is about 15,000 years, much longer than deep ocean mixing timescales, indicative of its role as a quasi-conservative oxyanion species.

In the upper 100 m, Sc and Ga replacement times are relatively short, roughly 10 years for both elements. Till et al. [2017] recently independently assessed the upper water column residence time of Sc as 5.6 ± 3.2 years near Bermuda, grossly consistent with the Th-based one, or perhaps suggesting the Sc/Th relatively solubility may be somewhat greater than 1, which would have reduced the Th-based estimate. The Ga replacement time is roughly consistent with the decadal-scale residence time inferred for this element in the North Atlantic (Shiller, 1998). The surface ocean Ba residence time of ~200 years is longer than the ~25 years estimated by Lea and Boyle [1991]. We are not aware of a good basis for comparison for the surface water replacement time estimates of V or Ni.

Finally, in Figure S5, we show the deep ocean residence time results based on the replacement time estimates for all elements considered in this study in the form of a periodic table, with comparison to available residence time estimates for most other elements in the periodic table. Note, as discussed

in the main text, replacement times are not necessarily equivalent to residence times, but we make that assumption here in order to see the overall pattern observed among the elements. A broad scale feature is apparent of long residence times for the left and right sides of the table (alkalis, alkali earths, and halogens) with short or intermediate residence times for the nonmetals, transition metals and lanthanides. Within the transition metals, there are interesting non-monotonic trends that, upon a more detailed analysis than attempted here, may provide further insights in the cycling of elements in the ocean.

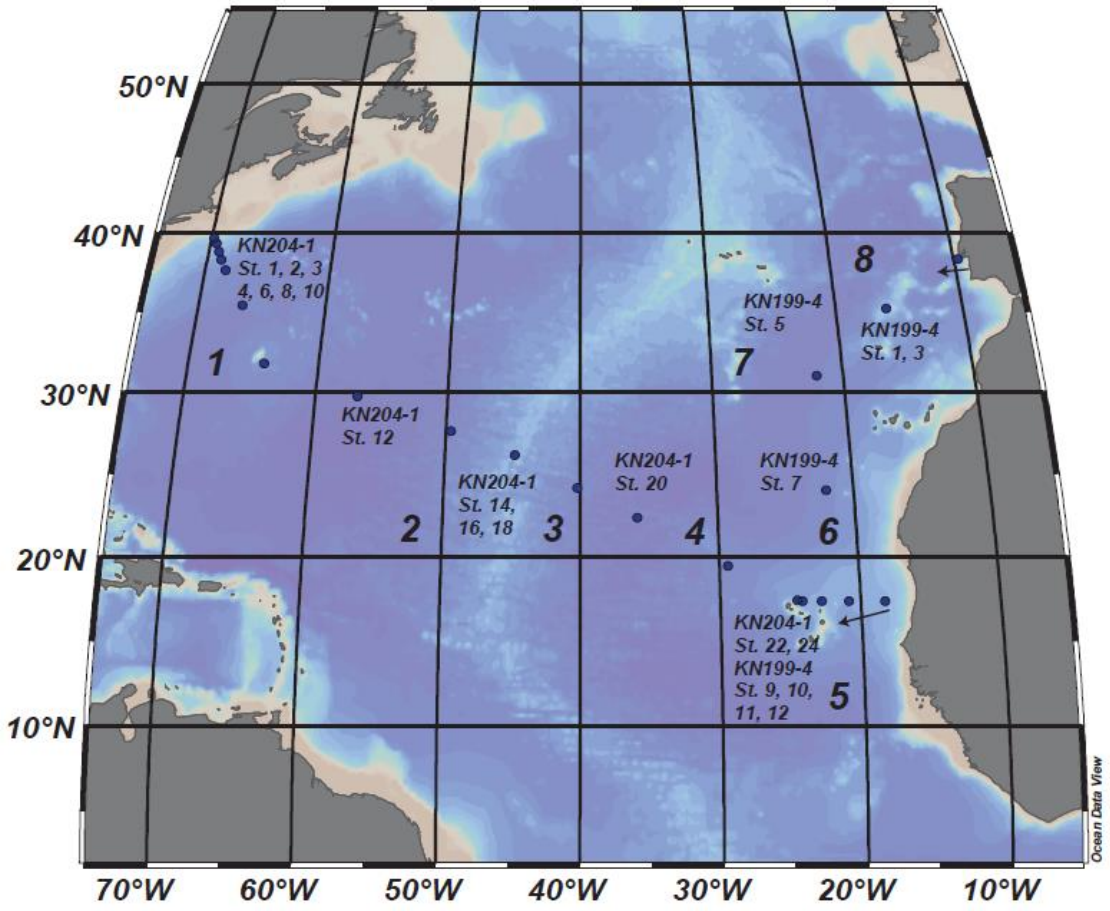

Figure S1. Location of GA03 stations for which replacement time estimates of trace elements can be made based on measured ^{232}Th supply. GA03 consisted of two cruises (KN199-4 from Portugal to Cape Verde and KN204-1 from Cape Cod to Cape Verde). To make a North Atlantic basin residence time estimate, the replacement time profiles at these stations were first binned into a common depth scheme. Depth bins were 0-100 m, 100-500 m, 500-1000 m, 1000-1500 m, 1500-2100 m, 2100-3000 m, 3000-4000 m, 4000-5000 m and 5000-5500 m, and were chosen to have at least one observation of ^{232}Th in each bin at each station. The station profiles within the 10° x 10° boxes labelled with a large number in the map (1 thru 8) were then averaged across depth bins. The averaged profiles from each numbered box were subsequently averaged with an area-weighting factor, taking into account the relative area of the different boxes. KN199-4 Station 1 on the Portuguese coast was averaged in Box 8 and KN199-4 St. 9 on the Mauritanian coast was averaged in Box 5.

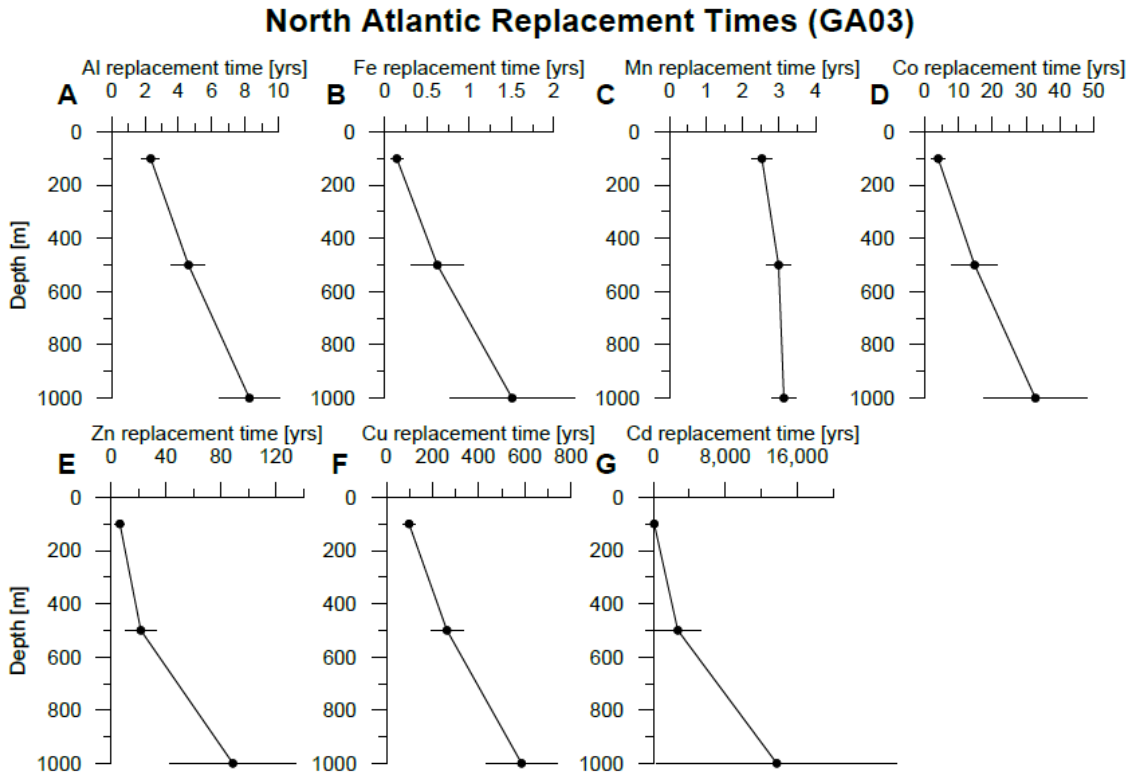

Figure S2. Residence time estimates in the upper 1000 m for dissolved elements with respect to dissolved ^{232}Th supply averaged for the North Atlantic basin using GA03 stations. The error bars represent the standard deviation of estimates arising from using either upper continental crustal or North African dust metal/thorium ratios and metal/thorium fractional solubility ratios defined by HAc or DI leaches of North African dust (Berger et al., 2008; Shelley et al., 2018).

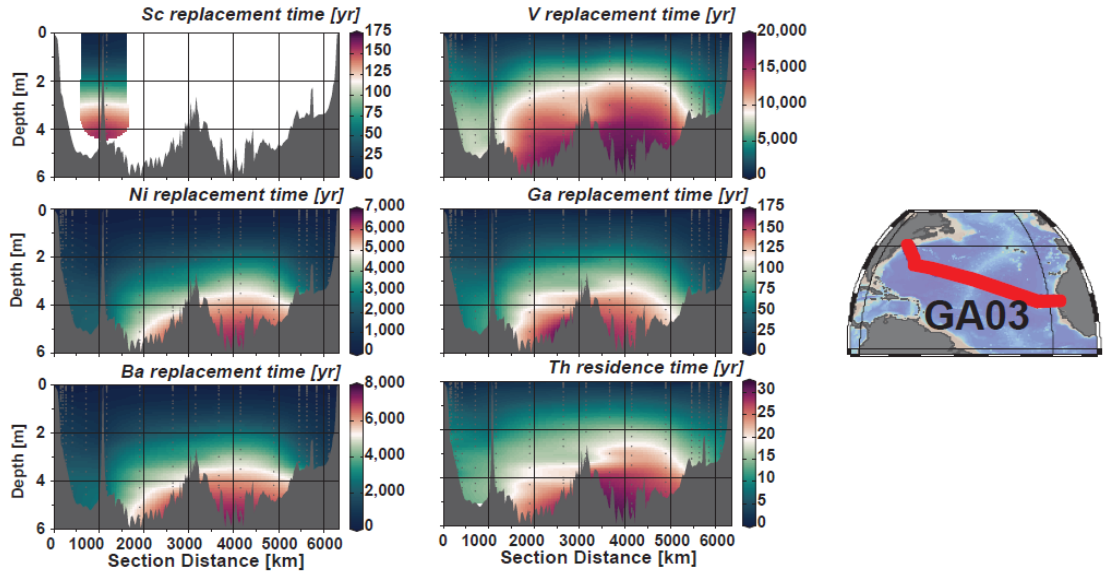

Figure S3. Replacement time estimates across the GA03 section for dissolved Sc, V, Ni, Ga, Ba and Th, with respect to dissolved ^{232}Th supply, upper continental crustal metal/thorium ratios (Rudnick and Gao, 2014) and metal/thorium fractional solubility ratios defined by deionized water leaches of North African dust (Table S1; Shelley et al., 2018). Dissolved Sc data were only available from 1 stations from GA03 (KN204-1 St. 10, co-located with BATS) (Parker et al., 2016). Data on dissolved V, Ni, Ga and Ba are published here for the first time, https://www.bco-dmo.org/dataset/3827). Th residence time is based on ^{230}Th scavenging which is considered in steady-state with supply by ^{234}U decay.

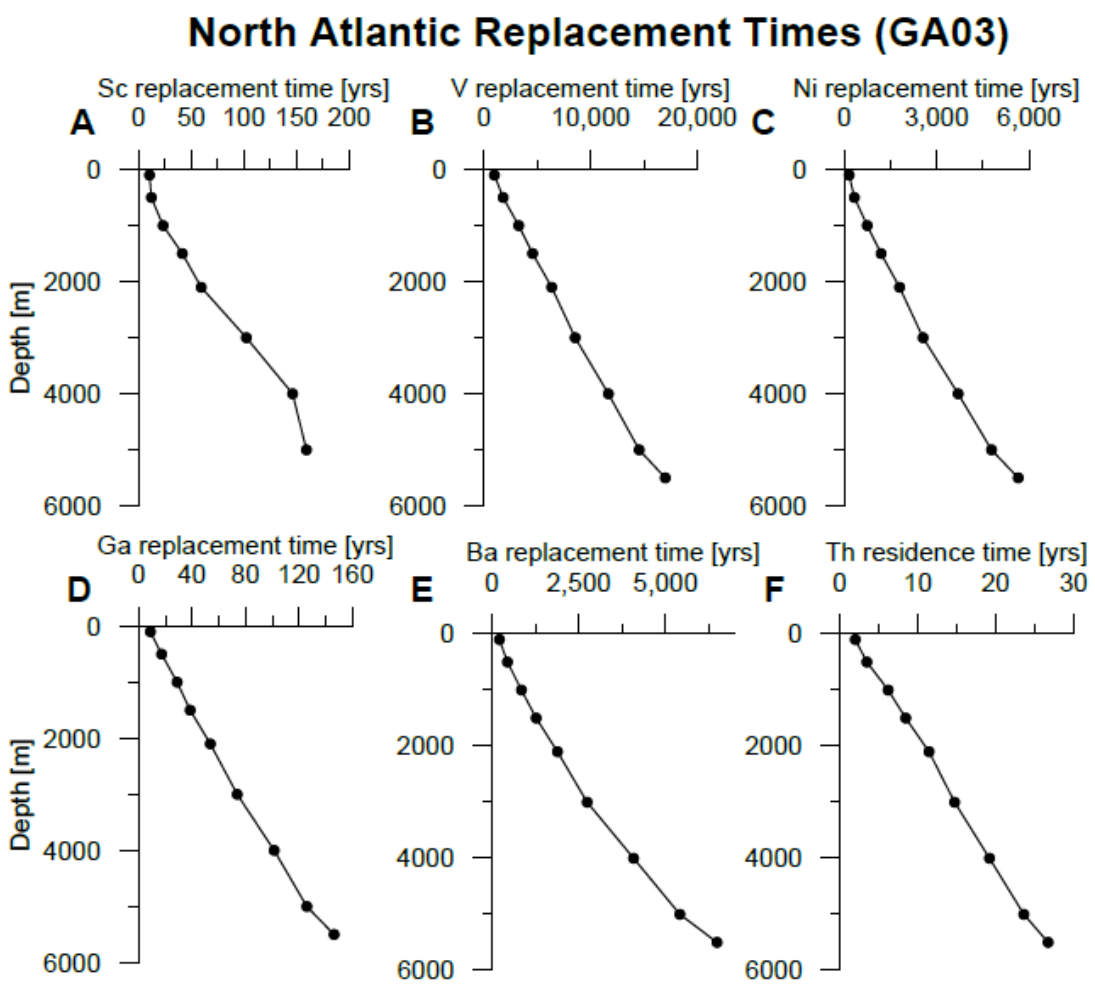

Figure S4. North Atlantic replacement time estimates for dissolved Sc, V, Ni, Ga and Ba, with respect to dissolved ^{232}Th supply, upper continental crustal metal/thorium ratios (Rudnick and Gao, 2014) and metal/thorium fractional solubility ratios defined by deionized water leaches of North African dust (Table S1; Shelley et al., 2018), or assumed (see Table 2). Dissolved Sc data were only available from 1 stations from GA03 (KN204-1 St. 10, co-located with BATS) (Parker et al., 2016); therefore, this profile is not a basin average but is likely representative of the subtropical gyre. Dissolved V, Ni, Ga and Ba data are published here for the first time (personal communication). Th residence time is based on ^{230}Th scavenging which is considered in steady-state with supply by ^{234}U decay.

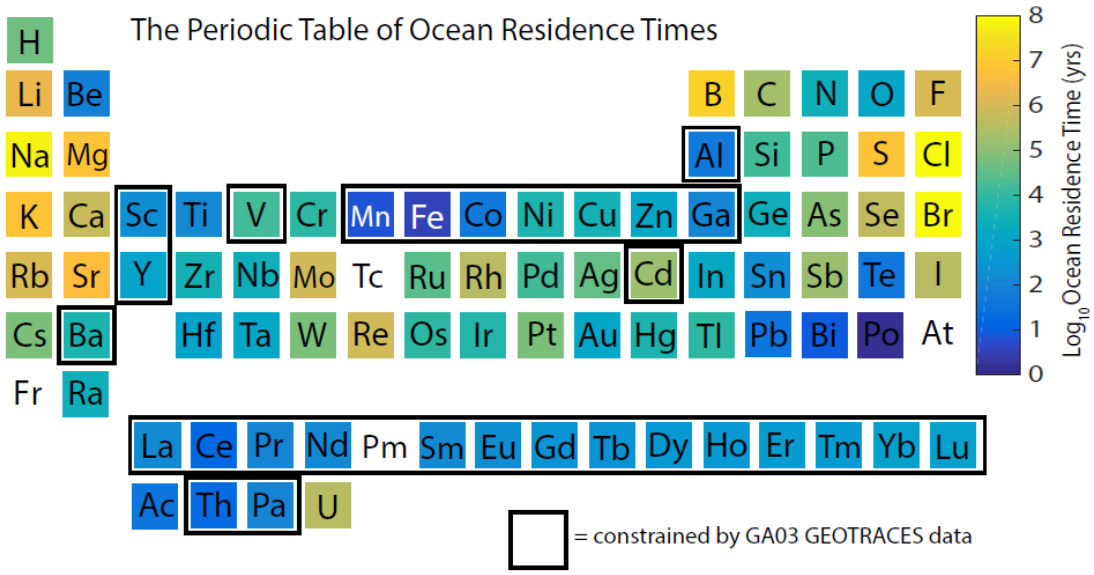

Figure S5. Residence times of the elements in the ocean, or the average time an element spends in the ocean between its supply and removal. New residence time estimates (outlined in black boxes) are based on the replacement times calculated in this study which were derived by comparing measurements of the element's dissolved inventory to its supply based on measured dissolved ^{232}Th supply integrated for the whole North Atlantic covered by GEOTRACES section GA03 (see main text for data citations), assuming an upper continental crustal (UCC) composition (Rudnick and Gao, 2014) of the material that supplies the elements and an informed estimate of the elemental solubility of UCC material based on deionized water leaches of North African dust aerosol samples (Shelley et al., 2018). The following references were used for the residence times of the other elements: H (as H_2O) (Berner and Berner, 2012); Li, B, Na, Mg, P (as dissolved inorganic phosphorous), S (as sulfate), Cl, K, and Ca: (Chester and Jickells, 2012); Be, F, Ge, As, Se, Rb, Ru, Pd, Ag, In, Sn, Sb, Se, Te, Cs, Ir, Pt, Hg, Tl and Bi: (Li, 1991); C (as dissolved inorganic carbon), N (as nitrate) and O (as molecular oxygen): (Broecker, 2015); Si (as dissolved inorganic silicon): (Sarmiento and Gruber, 2006); Sc (Parker et al., 2016); Ti: (Orians et al., 1990); Cr: (Reinhard et al., 2013); Br, Sr and I (as iodate): (Broecker and Peng, 1982); Zr, Nb, Hf and Ta (Firdaus et al., 2011); Mo and W: (Sohrin et al., 1998); Rh: (Bertine et al., 1993); Re: (Colodner et al., 2014); Os: (Oxburgh, 2001); Au: (Falkner and Edmond, 1990); and U: (Ku et al., 1977). Note that Tc and Pm (and the trans-uranics, not shown) are not naturally-occurring in the ocean and thus residence times are not given. Residence times of Po and At (and Fr and Ra, not shown) are limited by the length of their radioactive half-lives. Pb has been contaminated in the ocean by anthropogenic input and thus a steady-state residence time in not appropriate to define. The Pb residence time given (150-100 years) is based on residence times of ^{210}Pb with respect to scavenging derived by (Bacon et al., 1976). The noble gases are essentially non-reactive in the ocean, and therefore, these elements are not shown.

Table S1. Upper continental crust compositional ratios (Rudnick and Gao, 2014) and DI leach (Shelley et al., 2018) solubility ratios used in the residence time calculations presented above. The choice of these ratios is a large source of uncertainty in this method of estimating residence time based on thorium supply. Compositional ratios and solubility ratios are likely to differ for different sources (North African dust versus rivers versus hydrothermal vents, etc.). A more complete analysis of the sensitivity of these ratios to these factors is beyond the scope of this contribution.

	Sc	V	Ni	Ga	Ba
Me/Th (UCC) [mol/mol]	6.88	42.07	17.69	5.55	101.04
S_{Me}/S_{Th} (DI leach, or assumed; see supplementary text)	1 (assumed)	25 ±19 (n = 12)	29 ± 25 (n = 12)	5 (assumed)	12 ± 5 (n = 12)

References

Bacon, M.P., Spencer, D.W., Brewer, P.G., 1976. $^{210}Pb/^{226}Ra$ and $^{210}Po/^{210}Pb$ disequilibria in seawater and suspended particulate matter. Earth Planet. Sci. Lett. 32, 277–296. doi:10.1016/0012-821X(76)90068-6

Berger, C.J.M., Lippiatt, S.M., Lawrence, M.G., Bruland, K.W., 2008. Application of a chemical leach technique for estimating labile particulate aluminum, iron, and manganese in the Columbia River plume and coastal waters off Oregon and Washington. J. Geophys. Res. 113, C00B01. doi:10.1029/2007JC004703

Berner, E.K., Berner, R.A., 2012. Global Environment: Water, Air and Geochemical Cycles, Second Edi. ed. Princeton University Press, Princeton.

Bertine, K.K., Koide, M., Goldberg, E.D., 1993. Aspects of rhodium marine chemistry. Mar. Chem. 42, 199–210. doi:10.1016/0304-4203(93)90012-D

Broecker, W., 2015. Wally's Carbon World. Eldigio Press, Palisades, NY.

Broecker, W.S., Peng, T.-H., 1982. Tracers in the Sea. Eldigio Press, Palisades, NY.

Chan, L.H., Edmond, J.M., Stallard, R.F., Broecker, W.S., Chung, Y.C., Weiss, R.F., 1976. Radium and barium at GEOSECS stations in the Atlantic and Pacific. Earth Planet. Sci. Lett. 32, 258–267. doi:10.1016/0012-821X(76)90066-2

Chester, R., Jickells, T., 2012. Trace elements in the oceans, in: Marine Geochemistry. Blackwell Publishing Ltd, pp. 223–252. doi:10.1002/9781118349083

Colodner, D., Sachs, J., Ravizza, G., Turekian, K., Edmond, J., Boyle, E.A., 2014. The geochemical cycle of rhenium: a reconnaissance. Earth Planet. Sci. Lett. 117, 205–221. doi:10.1016/0012-821X(93)90127-U

Falkner, K.K., Edmond, J.M., 1990. Gold in seawater. Earth Planet. Sci. Lett. 98, 208–221. doi:10.1016/0012-821X(90)90060-B

Firdaus, M.L., Minami, T., Norisuye, K., Sohrin, Y., 2011. Strong elemental fractionation of Zr – Hf and Nb – Ta across the Pacific Ocean. Nat. Geosci. 4, 227–230. doi:10.1038/ngeo1114

Hayes, C.T., Fitzsimmons, J.N., Boyle, E.A., McGee, D., Anderson, R.F., Weisend, R., Morton, P.L., 2015. Thorium isotopes tracing the iron cycle at the Hawaii Ocean Time-series Station ALOHA. Geochim. Cosmochim. Acta 169, 1–16. doi:10.1016/j.gca.2015.07.019

Hayes, C.T., Rosen, J., McGee, D., Boyle, E.A., 2017. Thorium distributions in high- and low-dust regions and the significance for iron supply. Global Biogeochem. Cycles 31, 1–20. doi:10.1002/2016GB005511

Ku, T.L., Knauss, K.G., Mathieu, G.G., 1977. Uranium in open ocean: concentration and isotopic composition. Deep Sea Res. 24, 1005–1017. doi:10.1016/0146-6291(77)90571-9

Lea, D.W., Boyle, E.A., 1991. Barium in planktonic foraminifera. Geochim. Cosmochim. Acta 55, 3321–3331. doi:10.1016/0016-7037(91)90491-M

Li, Y.-H., 1991. Distribution patterns of the elements in the ocean: a synthesis. Geochim. Cosmochim. Acta 55, 3223–3240. doi:10.1016/0016-7037(91)90485-N

Measures, C.I., Brown, E.T., 1996. Estimating dust input to the Atlantic Ocean using surface water aluminum concentrations, in: Guerzoni, S., Chester, R. (Eds.), The Impact of Desert Dust Across the Mediterranean. Kluwer Academic Publishers, pp. 301–311. doi:10.1007/978-94-017-3354-0_30

Orians, K.J., Boyle, E.A., Bruland, K.W., 1990. Dissolved titantium in the open ocean. Nature 348, 322–325. doi:10.1038/348322a0

Oxburgh, R., 2001. Residence time of osmium in the oceans. Geochem Geophys Geosyst 2, 2000GC000104. doi:10.1029/2000GC000104

Parker, C.E., Brown, M.T., Bruland, K.W., 2016. Scandium in the open ocean: A comparison with other group 3 trivalent metals. Geophys. Res. Lett. 43, 2758–2764. doi:10.1002/2016GL067827

Rafter, P.A., Sigman, D.M., Mackey, K.R.M., 2017. Recycled iron fuels new production in the eastern equatorial Pacific Ocean. Nat. Commun. 8, 1100. doi:10.1038/s41467-017-01219-7

Reinhard, C.T., Planavsky, N.J., Robbins, L.J., Partin, C.A., Gill, B.C., Lalonde, S. V, Bekker, A., Konhauser, K.O., Lyons, T.W., 2013. Proterozoic ocean redox and biogeochemical stasis. Proc. Natl. Acad. Sci. U.S.A. 110, 5357–5362. doi:10.1073/pnas.1208622110

Rudnick, R.L., Gao, S., 2014. Composition of the Continental Crust, in: Holland, H.D., Turekian, K.K. (Eds.), Treatise on Geochemistry (Second Edition). Elsevier, Oxford, UK, doi: 10.1016/B978-0-08-095975-7.00301-6, pp. 1–51. doi:10.1016/B978-0-08-095975-7.00301-6

Sarmiento, J.L., Gruber, N., 2006. Ocean Biogeochemical Dynamics. Princeton University Press, Princeton.

Shelley, R.U., Landing, W.M., Ussher, S.J., Planquett, H., Sarthou, G., 2018. Characterisation of aerosol provenance from the fractional solubility of Fe (Al, Ti, Mn, Co, Ni, Cu, Zn , Cd and Pb) in North Atlantic aerosols (GEOTRACES GA01 and GA03). Biogeosciencess Disc. doi:10.5194/bg-2017-415

Shelley, R.U., Morton, P.L., Landing, W.M., 2015. Elemental ratios and enrichment factors in aerosols from the US-GEOTRACES North Atlantic transects. Deep Sea Res. II 116, 262–272. doi:10.1016/j.dsr2.2014.12.005

Shiller, A.M., 1998. Dissolved gallium in the Atlantic Ocean. Mar. Chem. 61, 87–99. doi:10.1016/S0304-4203(98)00009-7

Shiller, A.M., Bairamadgi, G.R., 2006. Dissolved gallium in the northwest Pacific and the south central Atlantic Ocean: Implications for aeolian Fe input and a reconsideration of profiles. Geochemistry Geophys. Geosystems 7, Q08M09. doi:10.1029/2005GC001118

Sohrin, Y., Fujishima, Y., Ueda, K., Akiyama, S., Mori, K., Hasegawa, H., Matsui, M., 1998. Dissolved niobium and tantalum in the North Pacific. Geophys. Res. Lett. 25, 999–1002. doi:10.1029/98GL00646

Till, C.P., Shelley, R.U., Landing, W.M., Bruland, K.W., 2017. Dissolved scandium, yttrium, and lanthanum in the surface waters of the North Atlantic: Potential use as an indicator of scavenging

intensity. J. Geophys. Res. Ocean. 122, 1–14. doi:10.1002/2017JC012696

Trapp, J.M., Millero, F.J., Prospero, J.M., 2010. Temporal variability of the elemental composition of African dust measured in trade wind aerosols at Barbados and Miami. Mar. Chem. 120, 71–82. doi:10.1016/j.marchem.2008.10.004